

Supporting Information

Synthesis and structure of thienyl Fischer carbene complexes of Pt^{II} for application in alkyne hydrosilylation

Zandria Lamprecht,^a Frederick P. Malan,^a Simon Lotz,^a and Daniela I. Bezuidenhout*^b

^a *Department of Chemistry, University of Pretoria, Private Bag X20, Hatfield 0028, Pretoria, South Africa*

^b *Laboratory of Inorganic Chemistry, Environmental and Chemical Engineering, University of Oulu, P. O. Box 3000, 90014 Oulu, Finland*

*Email: daniela.bezuidenhout@oulu.fi

Table of Contents

S1. Precursor and complex synthesis details	S2
S2. ¹ H and ¹³ C NMR spectra	S4
S3. 2D NMR spectroscopy	S11
S4. Molecular structures, crystal data collection and structure refinement parameters	S13
S5. Crystal packing	S16
S6. Hydrosilylation catalysis	S18
S7. ESI-MS	S26
S8. References	S28

S1. Precursor and complex synthesis details

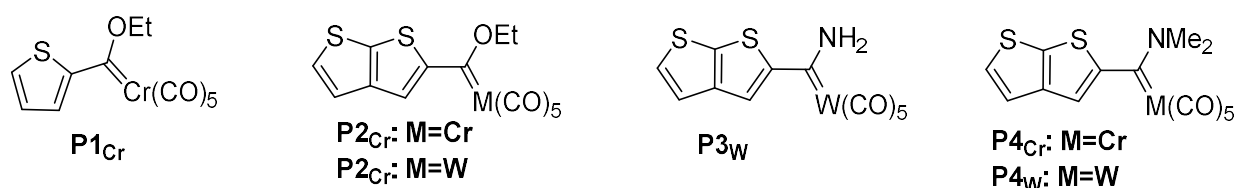
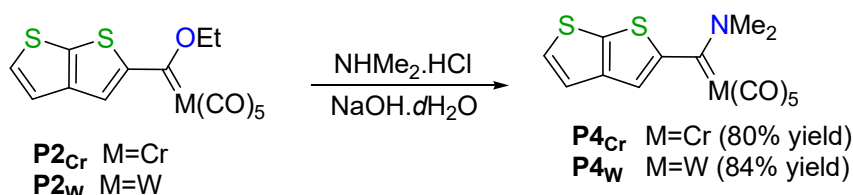


Fig. S1. Group 6 FCCs employed as precursor complexes

Aminolysis of chromium and tungsten monocarbene complexes of thieno[2,3-*b*]thiophene using dimethylamine hydrochloride

Compounds **P2_{Cr}** and **P2_W** are aminolysed, using a method previously reported by us.¹ [Cr(CO)₅{C(NMe₂)-5-C₆H₃S₂}] (**P4_{Cr}**, 80%) and [W(CO)₅{C(NMe₂)-5-C₆H₃S₂}] (**P4_W**, 84%) are obtained in good yield from two separate reactions.



Scheme S1. Synthesis of group 6 FCC precursors **P4**

Compounds **P2_{Cr}** (1.26 g, 3.3 mmol) and **P2_W** (0.37 g, 0.7 mmol) were each independently dissolved in 10 mL THF. Dimethylamine hydrochloride (2.45 g (30.0 mmol) and 0.58 g (7.1 mmol), respectively) and sodium hydroxide (1.20 g (30.0 mmol) and 0.28 g (7.1 mmol), respectively) were added to the reactions. Distilled H₂O was added dropwise until all the suspended salts were dissolved and a colour change observed. The reactions were followed with TLC until all the starting material had reacted. The reaction mixtures were extracted with ether and each reaction's combined ether layers washed with distilled H₂O saturated with NHMe₂.HCl. Afterwards the ether layers were dried over MgSO₄, filtered and the solvent reduced *in vacuo*. The products were purified using column chromatography starting with *n*-hexane and then increasing the polarity with DCM. From each reaction only one product was isolated and is listed in Table S1.

Table S1. Yields and colours of complex products

Compound	Name	Mass (g)	Yield (%)	Colour
P4_{Cr}	[Cr(CO) ₅ {C(NMe ₂)-5-C ₆ H ₃ S ₂ }]	1.00	80	Yellow
P4_W	[W(CO) ₅ {C(NMe ₂)-5-C ₆ H ₃ S ₂ }]	0.31	84	Yellow

P4_{Cr}: $\lambda_{\max}(\text{CH}_2\text{Cl}_2)/\text{nm}$ 380 ($\epsilon/\text{dm}^3 \text{ mol}^{-1} \text{ cm}^{-1}$ 4760). $\nu_{\text{CO}}(\text{hexane})/\text{cm}^{-1}$ 2056m ($A_1^{(1)}$), 1977w (B_1), 1941s ($A_1^{(2)}$ and E). $\delta^1\text{H}$ (400.13 MHz; CDCl_3 ; Me_4Si) 6.66 (1 H, s, H4), 7.30 (1 H, d, $^3J_{5',4'}$ 5.0, H5'), 7.19 (1 H, d, $^3J_{4',5'}$ 5.0, H4'), 4.02 and 3.31 (3 H + 3 H, s, CH_3). $\delta^{13}\text{C}$ (100.613 MHz; CDCl_3 ; Me_4Si) 268.9 (C_{carb}), 223.6 (CO_{trans}), 216.7 (CO_{cis}), 154.7 (C5), 110.5 (C4), 146.5 and 136.3 (C3 and C2), 128.0 ($C5'$), 120.3 ($C4'$), 51.4 and 46.9 (NMe_2).

P4_w: $\lambda_{\max}(\text{CH}_2\text{Cl}_2)/\text{nm}$ 350 ($\epsilon/\text{dm}^3 \text{ mol}^{-1} \text{ cm}^{-1}$ 6800). $\nu_{\text{CO}}(\text{hexane})/\text{cm}^{-1}$ 2064m ($A_1^{(1)}$), 1975w (B_1), 1940s (E), 1933s, sh ($A_1^{(2)}$). $\delta^1\text{H}$ (300.13 MHz; CDCl_3 ; Me_4Si) 6.71 (1 H, s, H4), 7.31 (1 H, d, $^3J_{5',4'}$ 5.2, H5'), 7.20 (1 H, d, $^3J_{4',5'}$ 5.2, H4'), 3.95 and 3.30 (3 H + 3 H, s, CH_3). $\delta^{13}\text{C}$ (75.468 MHz; CDCl_3 ; Me_4Si) 249.8 (C_{carb}), 203.7 (CO_{trans}), 198.2 (CO_{cis}), 156.1 (C5), 111.3 (C4), 146.3 and 136.6 (C3 and C2), 128.1 ($C5'$), 120.3 ($C4'$), 53.8 and 45.4 (NMe_2). $m/z(\text{C}_{14}\text{H}_9\text{O}_5\text{NS}_2\text{W}$, 519.19 g/mol) calculated: 569.8666, found: 569.8348 (31%, $[\text{M}+\text{Br}-\text{CO}]^-$), calculated: 541.8717, found: 541.8394 (14%, $[\text{M}+\text{Br}-2\text{CO}]^-$).

Table S2. Yields and colours of complex products obtained from the synthesis of 1

Compound	Name	Mass (g)	Yield (%)	Colour
P1_{Cr}	$[\text{Cr}(\text{CO})_5\{\text{C}(\text{OEt})-2-\text{C}_4\text{H}_3\text{S}\}]$	0.57	19	Orange
Pt(COD)Cl₂	Pt(COD)Cl ₂	0.58	38	White
1	<i>cis</i> - $[\text{PtCl}_2\{\text{C}(\text{OEt})-2-\text{C}_4\text{H}_3\text{S}\}_2]$	1.19	53	Yellow

Table S3. Yields and colours of complex products obtained from the synthesis of 2

Compound	Name	Mass (g)	Yield (%)	Colour
P2_{Cr}	$[\text{Cr}(\text{CO})_5\{\text{C}(\text{OEt})-5-\text{C}_6\text{H}_3\text{S}_2\}]$	0.11	67	Red
Pt(COD)Cl₂	Pt(COD)Cl ₂	0.010	17	White
2	<i>cis</i> - $[\text{PtCl}_2\{\text{C}(\text{OEt})-5-\text{C}_6\text{H}_3\text{S}_2\}_2]$	0.034	35	Yellow-brown

Table S4. Yields and colours of complex products obtained from the synthesis of 3

Compound	Name	Mass (g)	Yield (%)	Colour
P3_w	$[\text{W}(\text{CO})_5\{\text{C}(\text{NH}_2)-5-\text{C}_6\text{H}_3\text{S}_2\}]$	0.044	41	Yellow
3a	<i>cis</i> - $[\text{PtCl}_2\{\text{C}(\text{NH}_2)-5-\text{C}_6\text{H}_3\text{S}_2\}_2]$	0.027	64	Yellow
3b	<i>cis</i> - $[\text{PtCl}_2\{\text{C}(\text{NH}_2)-5-\text{C}_6\text{H}_3\text{S}_2\}_2]$		13	Yellow

Table S5. Yields and colours of complex products obtained from the synthesis of 4

Compound	Name	Mass (g)	Yield (%)	Colour
P4_{Cr}	$[\text{Cr}(\text{CO})_5\{\text{C}(\text{NMe}_2)-5-\text{C}_6\text{H}_3\text{S}_2\}]$	0.006	4	Yellow
4a	<i>cis</i> - $[\text{PtCl}_2\{\text{C}(\text{NMe}_2)-5-\text{C}_6\text{H}_3\text{S}_2\}_2]$		39	White-yellow
4b	<i>cis</i> - $[\text{PtCl}_2\{\text{C}(\text{NMe}_2)-5-\text{C}_6\text{H}_3\text{S}_2\}_2]$	0.103	8	White-yellow
4d	$[\text{PtCl}\{\text{C}(\text{NMe}_2)-5-\text{C}_6\text{H}_3\text{S}_2\}_3]^+\text{Cl}^-$		24	White-yellow
5	$(\text{NMe}_2)\text{C}(\text{O})-5-\text{C}_6\text{H}_3\text{S}_2$	0.023	24	White

S2. ^1H and ^{13}C NMR spectra

For NMR active Pt compounds Pt—C coupling, in the form of a singlet (C_{carb}) with a pair of platinum satellites, is expected with 1J (^{13}C — ^{195}Pt) ranging from 677—966 Hz.^{2,3} In this study, the low signal to noise ratio in the ^{13}C NMR spectra precludes the observation of the low intensity satellite peaks of the observed singlet resonances.

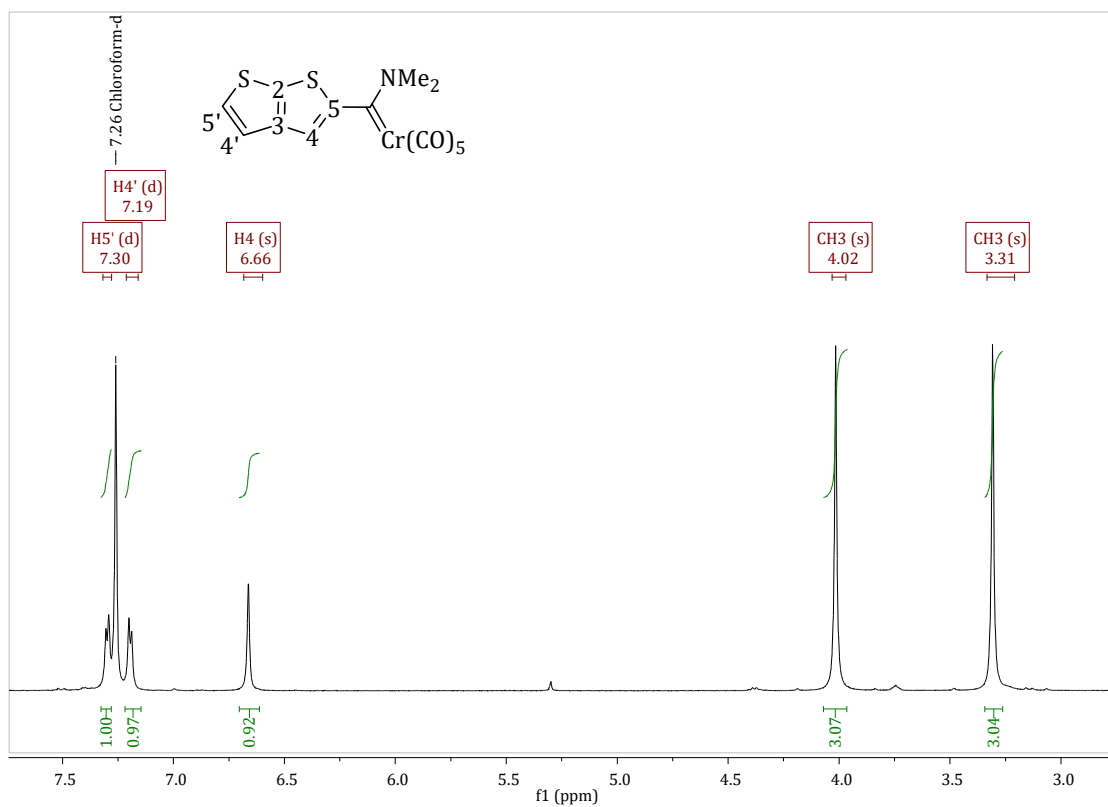


Fig. S2 ^1H NMR spectrum of P4_{Cr} in CDCl_3

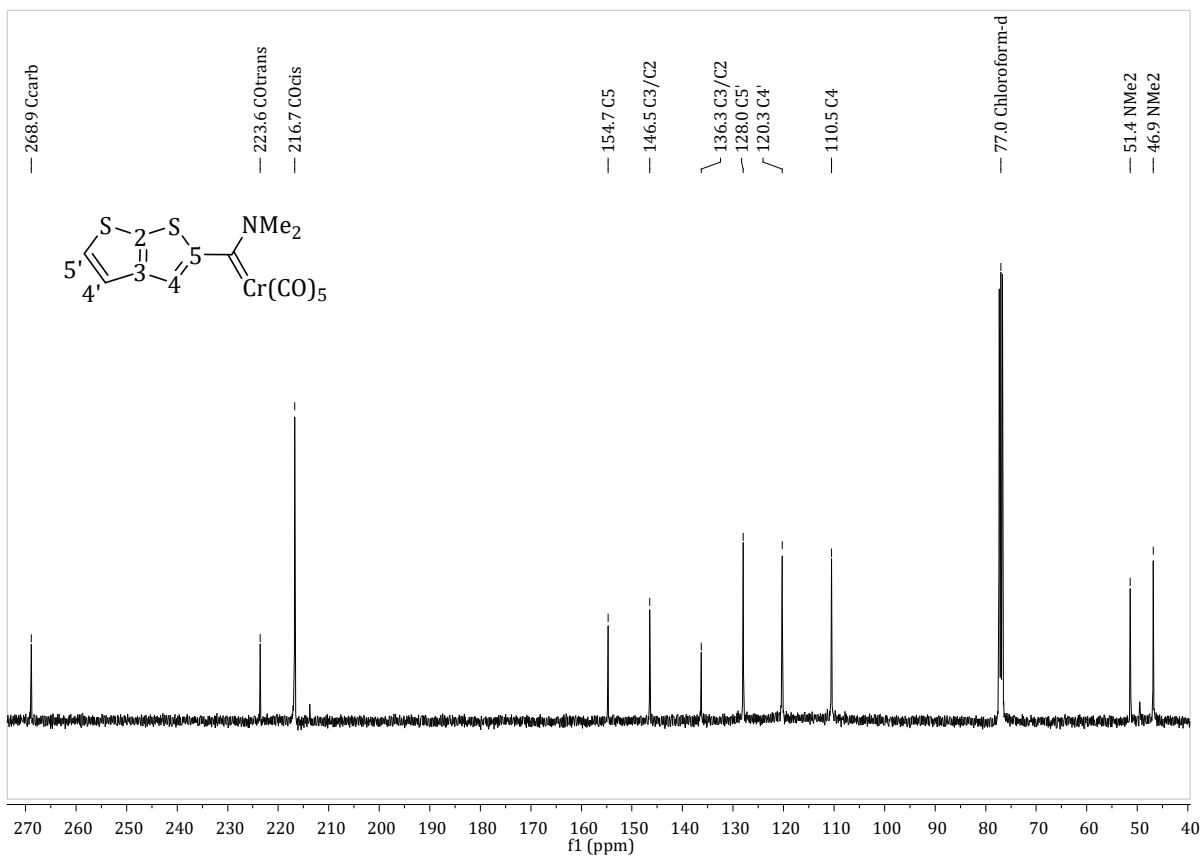


Fig. S3 ¹³C NMR spectrum of **P4_{Cr}** in CDCl₃

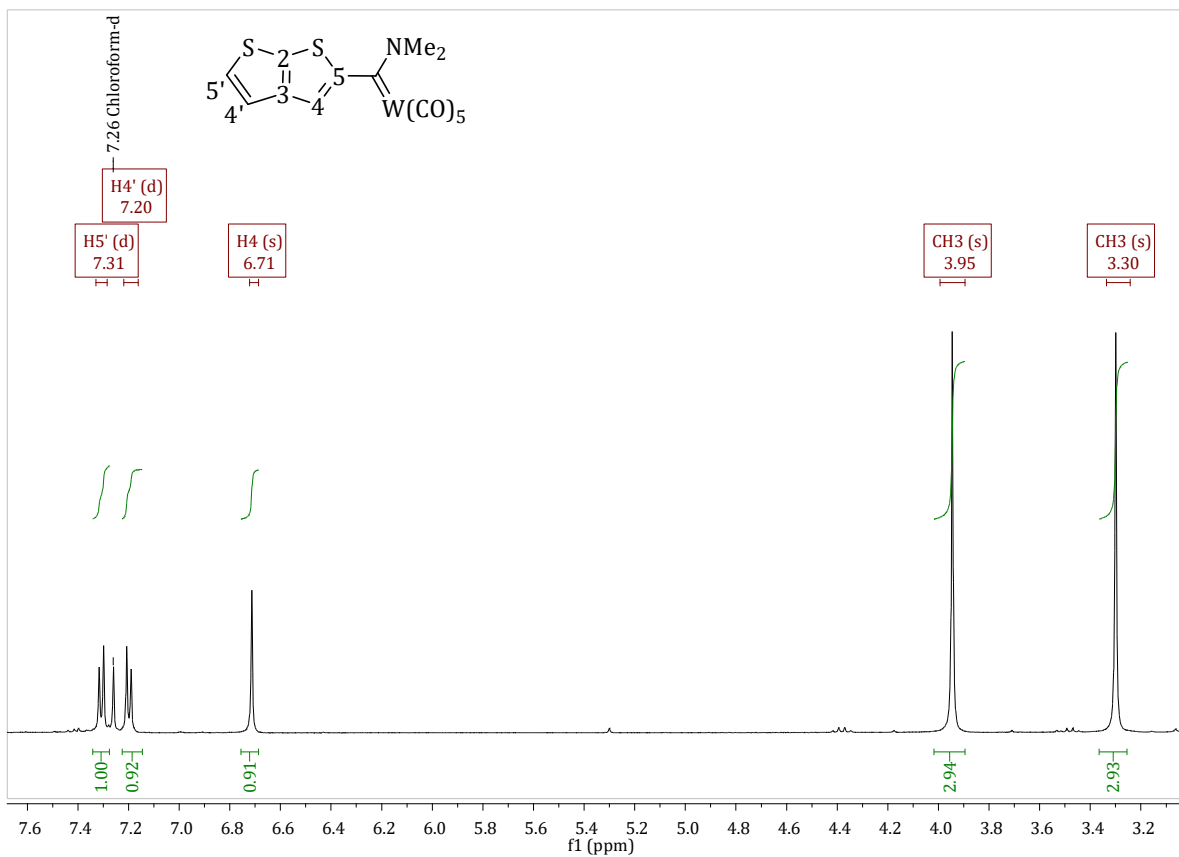


Fig. S4 ¹H NMR spectrum of **P4_W** in CDCl₃

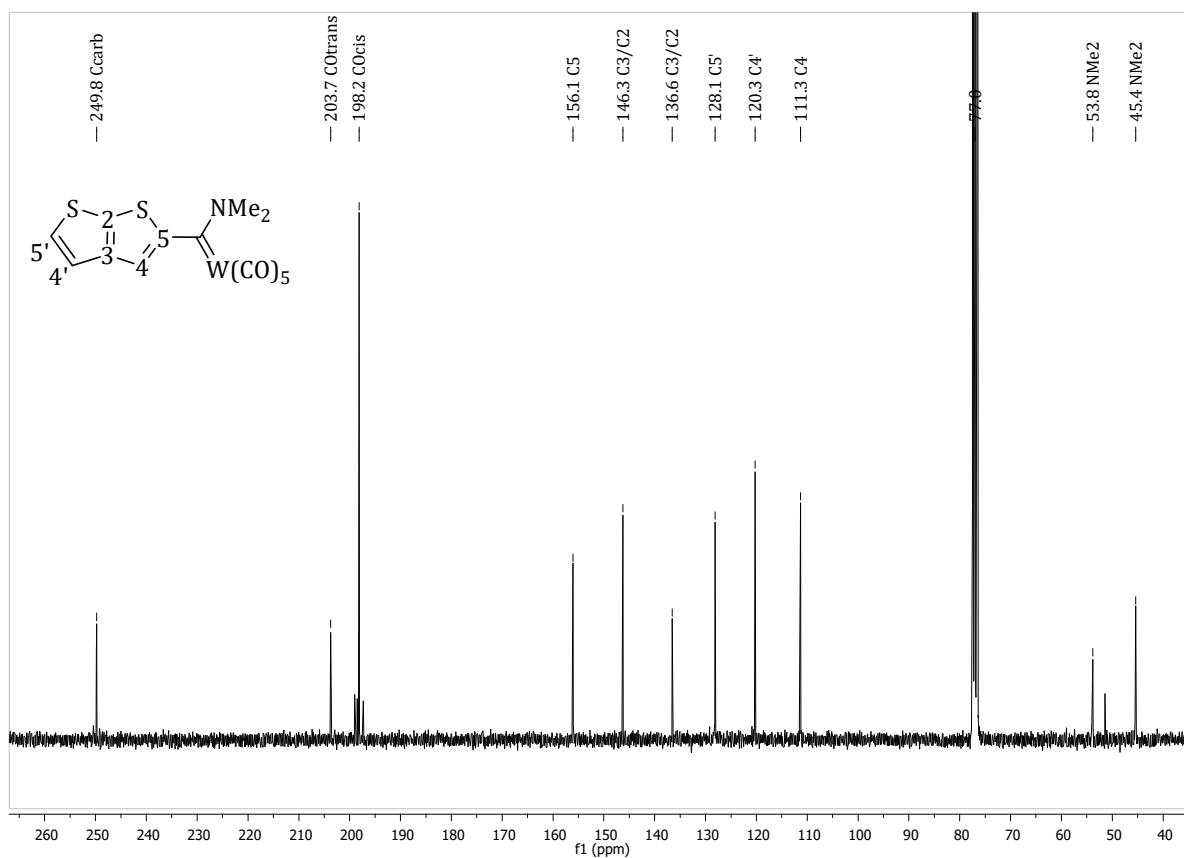


Fig. S5 ^{13}C NMR spectrum of **P4w** in CDCl_3

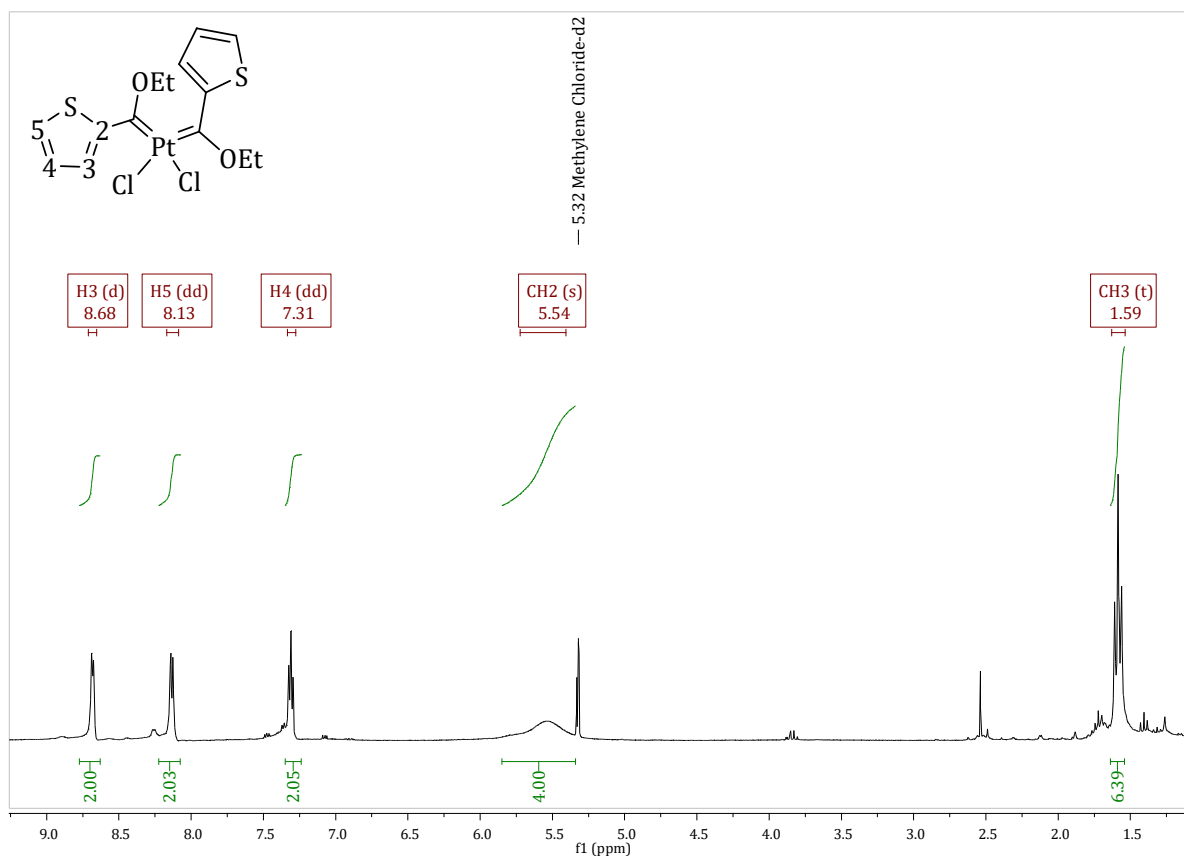


Fig. S6 ^1H NMR spectrum of **1** in CD_2Cl_2

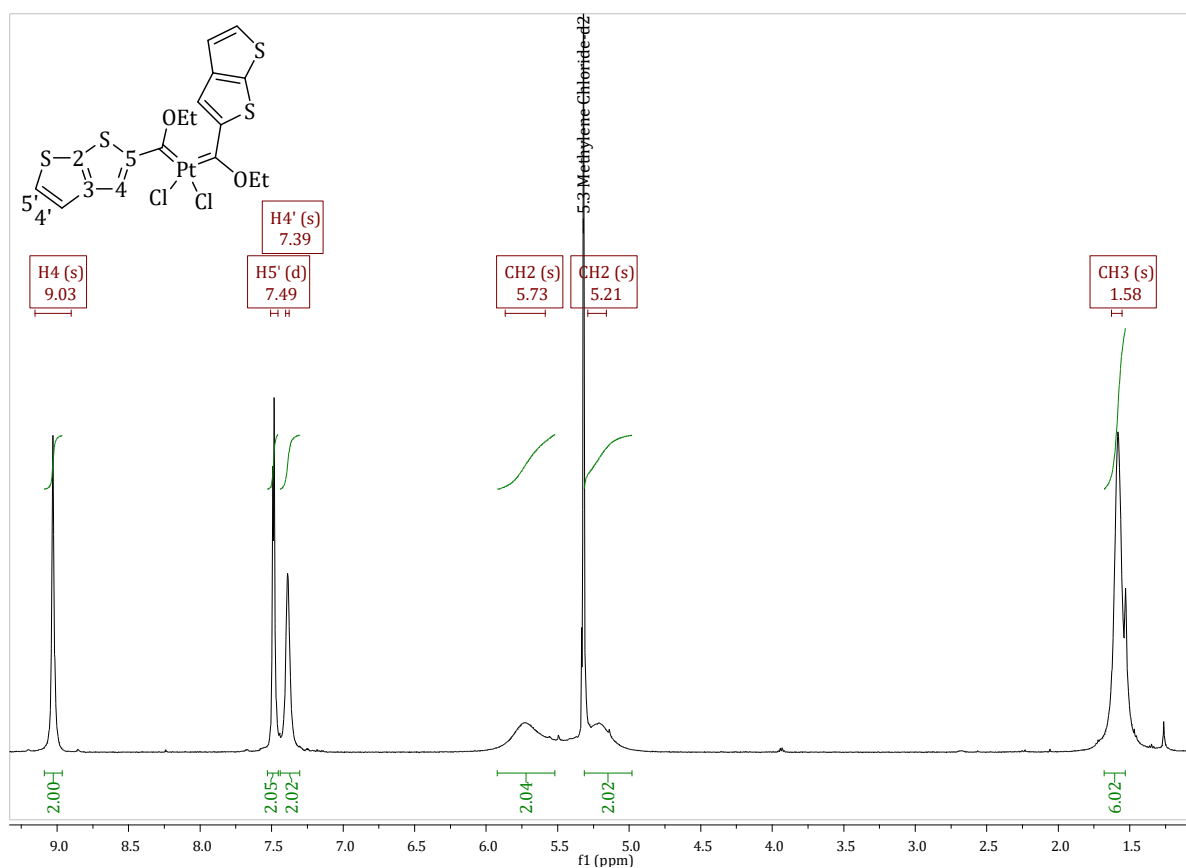


Fig. S7 ^1H NMR spectrum of **2** in CD_2Cl_2

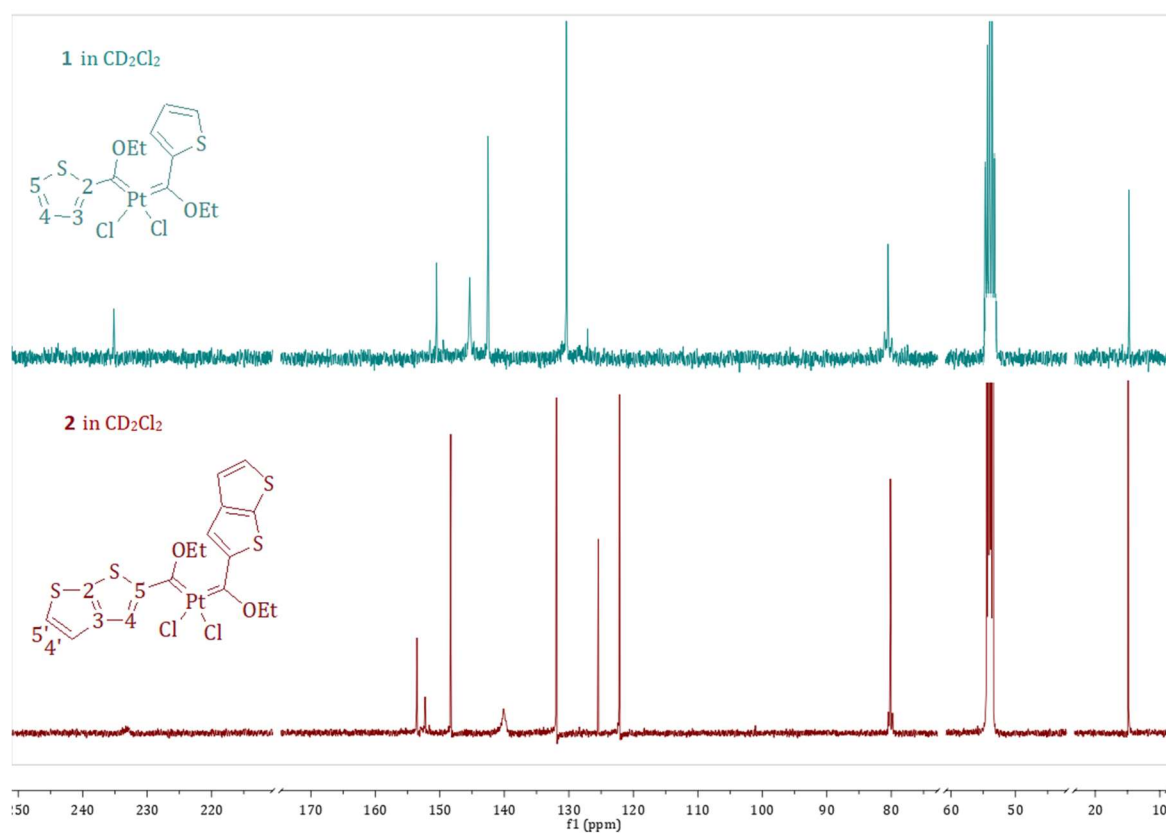


Fig. S8 ^{13}C NMR spectra showing chemical shift patterns for **1** and **2** in CD_2Cl_2

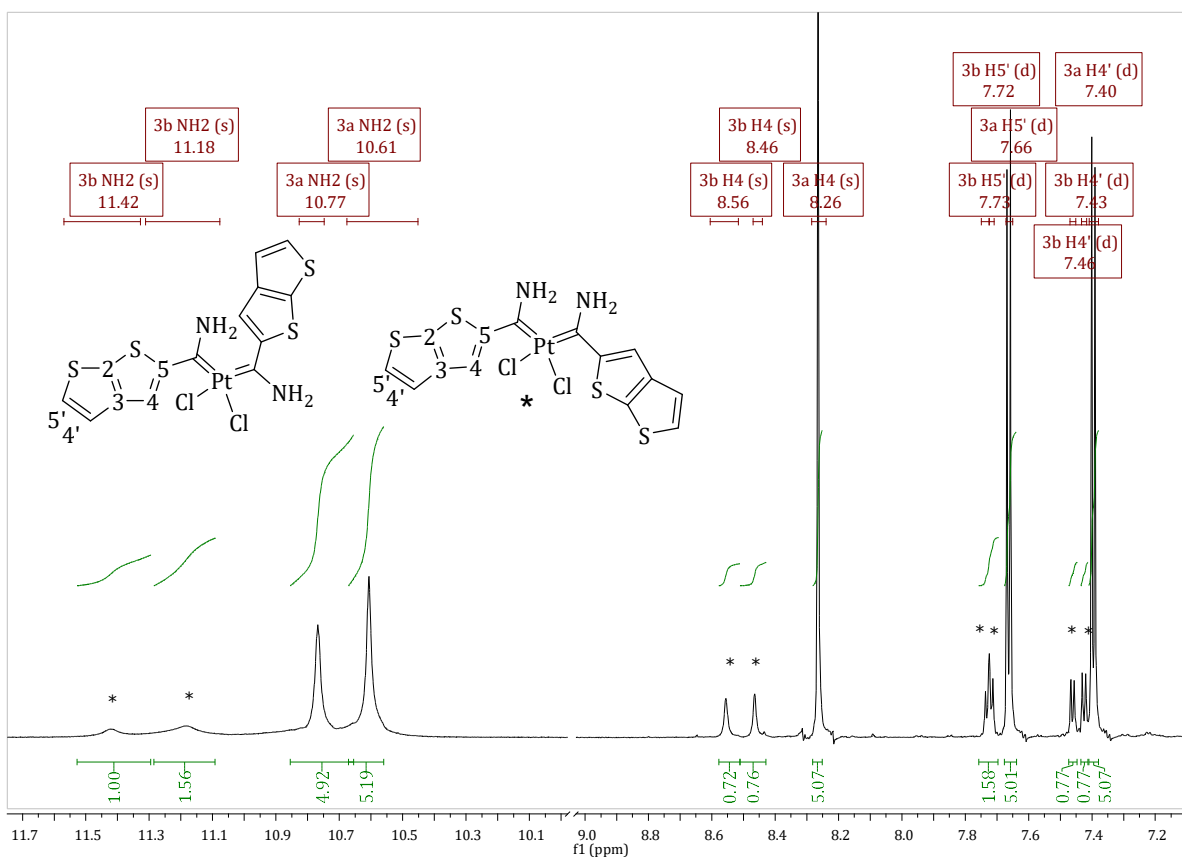


Fig. S9 ¹H NMR spectrum of **3a** and **3b*** in (CD₃)₂SO

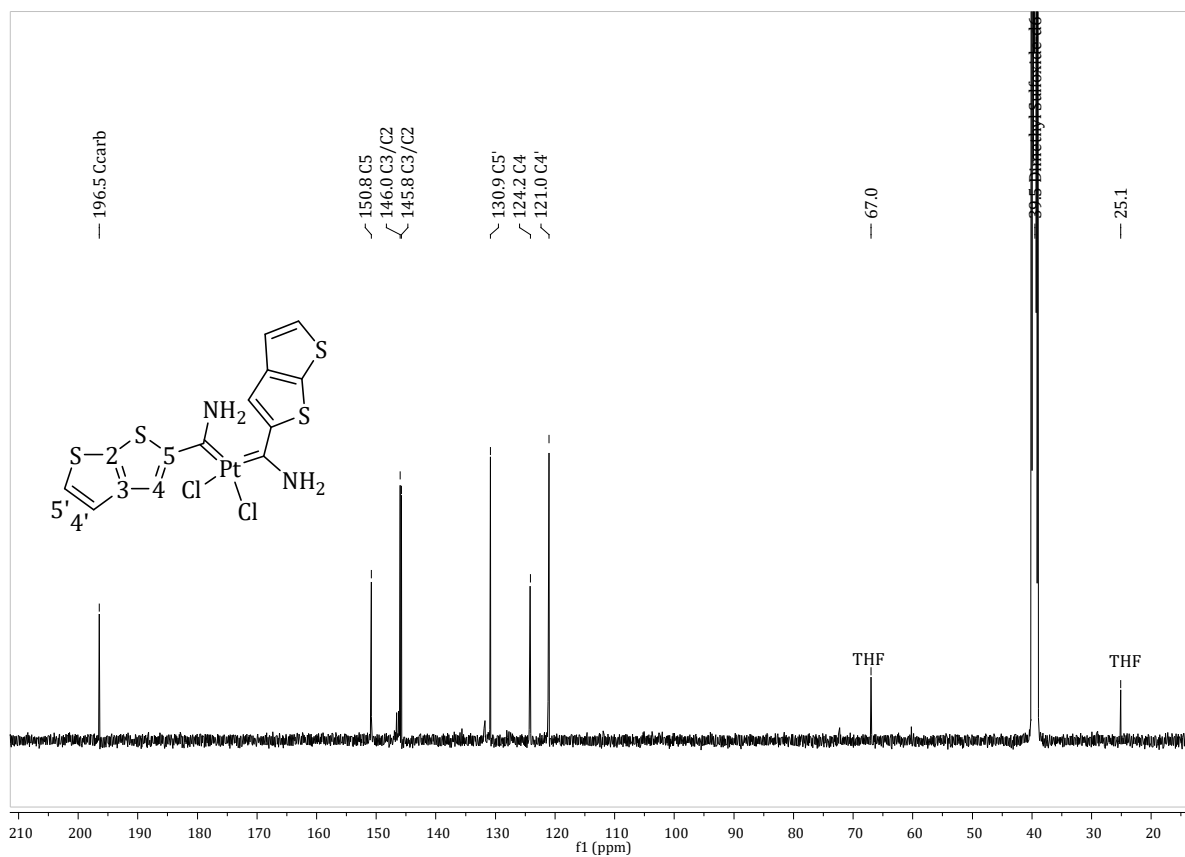


Fig. S10 ¹³C NMR spectrum of **3a** in (CD₃)₂SO

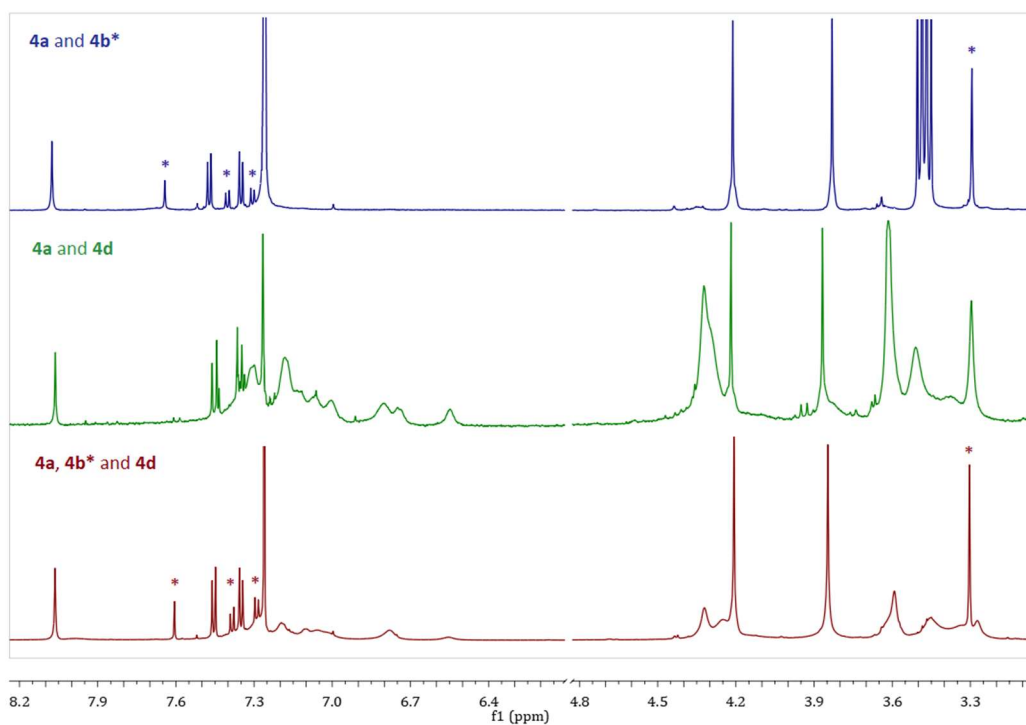


Fig. S11 ^1H NMR spectra showing chemical shift patterns for **4a**, **4b** and **4d** as mixtures in CDCl_3

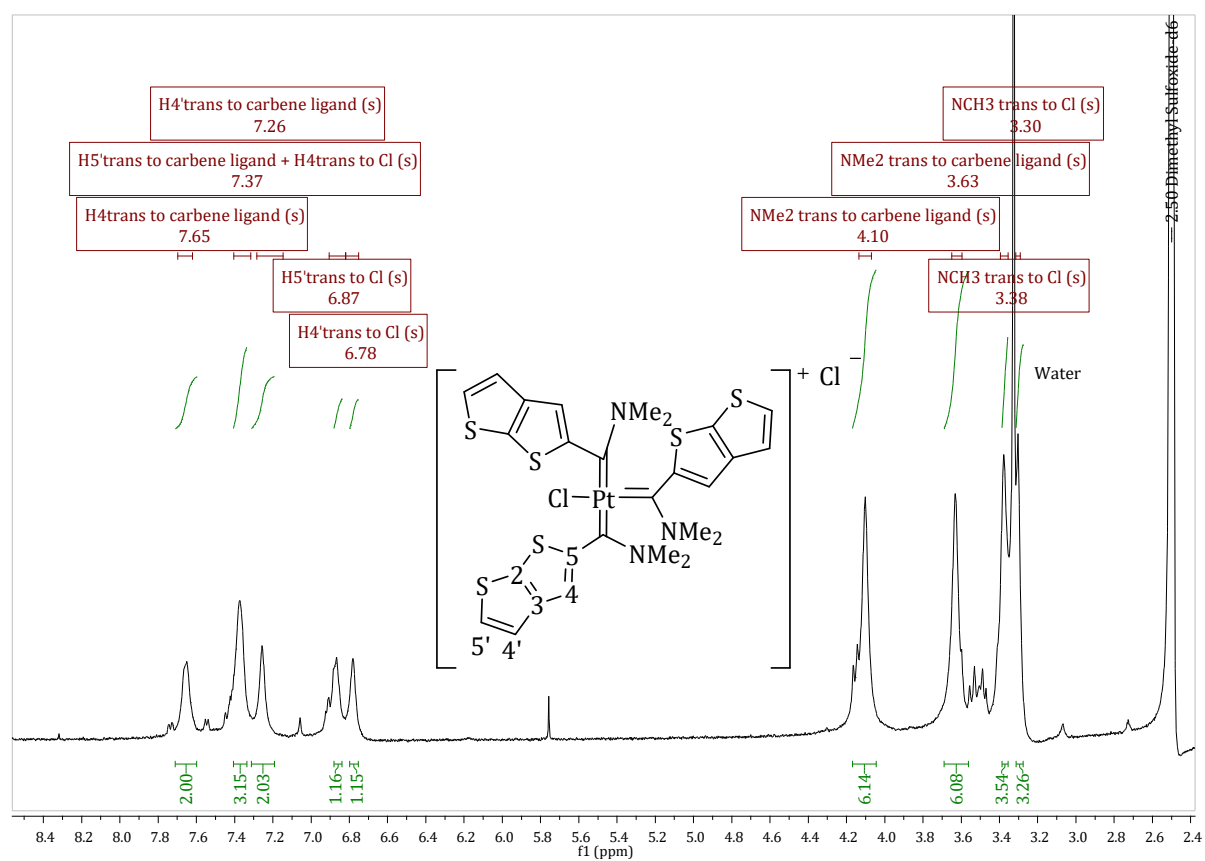


Fig. S12 ^1H NMR spectrum of **4d** in $(\text{CD}_3)_2\text{SO}$

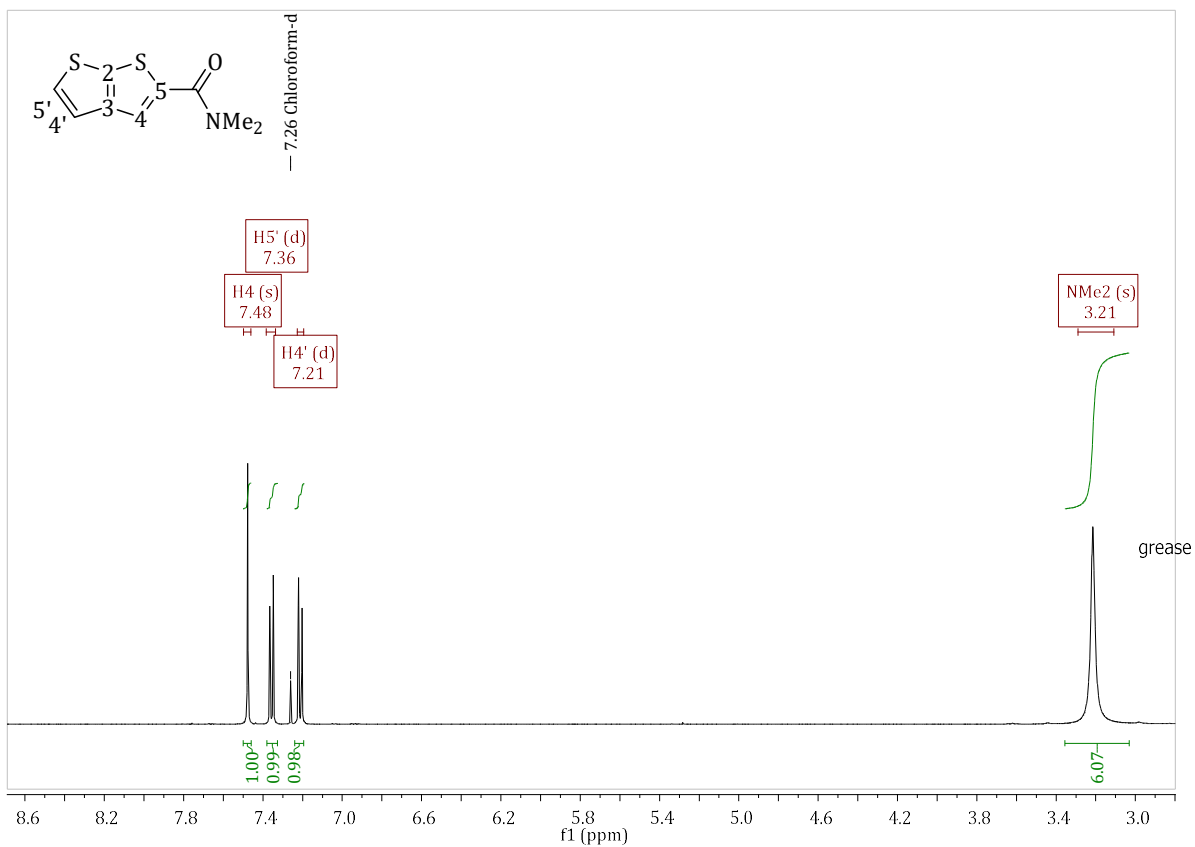


Fig. S13 ¹H NMR spectrum of 5 in CDCl₃

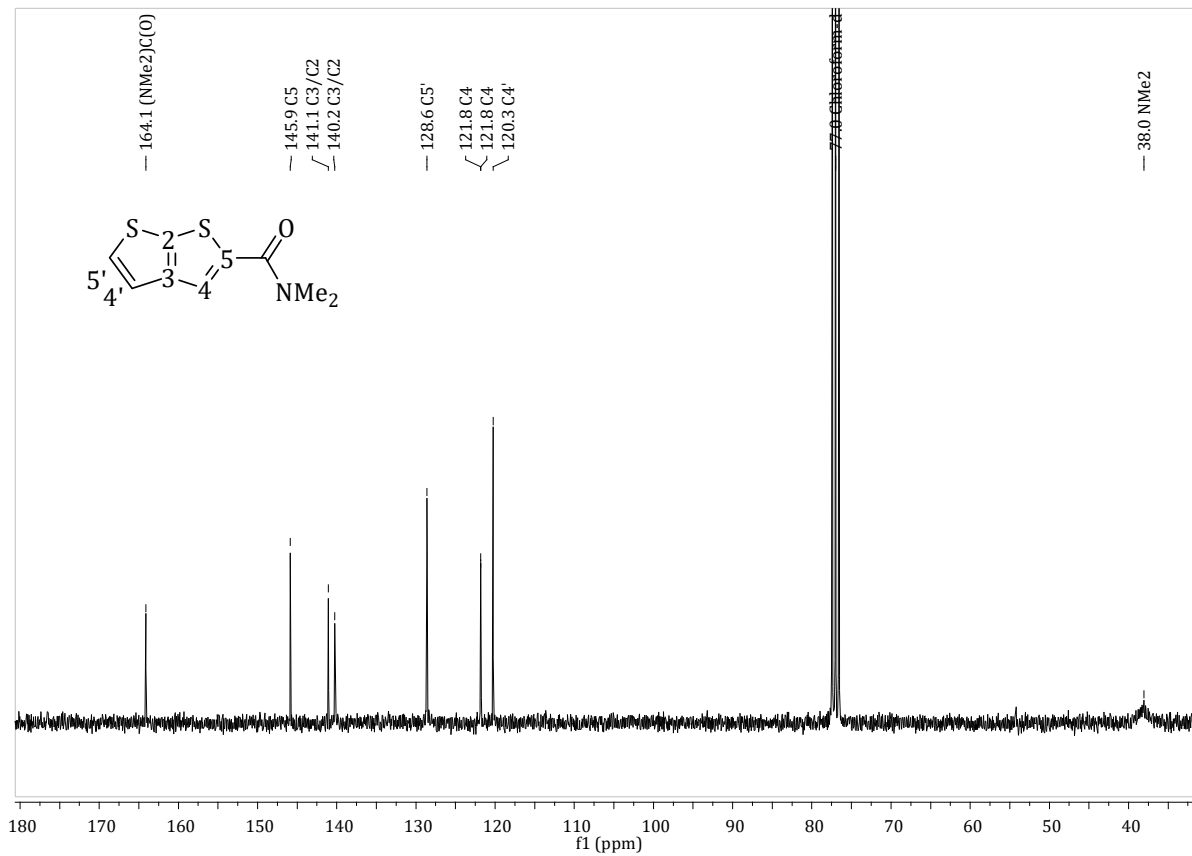


Fig. S14 ¹³C NMR spectrum of 5 in CDCl₃

S3. 2D NMR spectra

Aromatic protons of **1** are assigned by considering their ^1H NMR coupling constants. The order of aromatic resonances, proton and carbon, for **1** is confirmed using a $[^1\text{H}, ^{13}\text{C}]$ HSQC NMR spectrum (Fig. S15). As expected the order from most downfield is: H/C3 > H/C5 > H/C4. The HSQC NMR spectral measurement is also required to confirm the assignment of the broad proton signal as the methylene group. Through interpretation of the $[^1\text{H}, ^{13}\text{C}]$ HMBC NMR spectrum, the C2 and C_{carb} quaternary carbons are assigned (Fig. S16). From the HMBC NMR spectrum the methylene assignment is again confirmed through the couplings of methyl (1.59 ppm) to the methylene resonance (80.5 ppm).

The order of aromatic protons of ethoxy- and amino-[2,3-*b*]-TT carbene complexes, **2** – **5**, from most downfield is: H4 > H5' > H4'. The same trend is seen in their aromatic carbons, C4 > C5' > C4', with the exception of **3a** and **5**. In the case of **3a** and **5**, the trend is determined by means of a HSQC NMR spectrum to be C5' > C4 > C4' (Fig. S17 for **3a**). The HMBC NMR spectrum of **3a** confirms the trend (Fig. S18). Interestingly, both NH signals couple with the *ipso* carbon (C5) in the HMBC NMR spectrum of **3a**, but only the most downfield NH resonance coupled with the carbene carbon.

Assignments cannot be made unambiguously for the aromatic quaternary carbons, C2 and C3, of **2**–**5**. Not even the HMBC NMR spectra could assist with the assignments as these two carbons resonate too close together for resolution (Fig. S18).

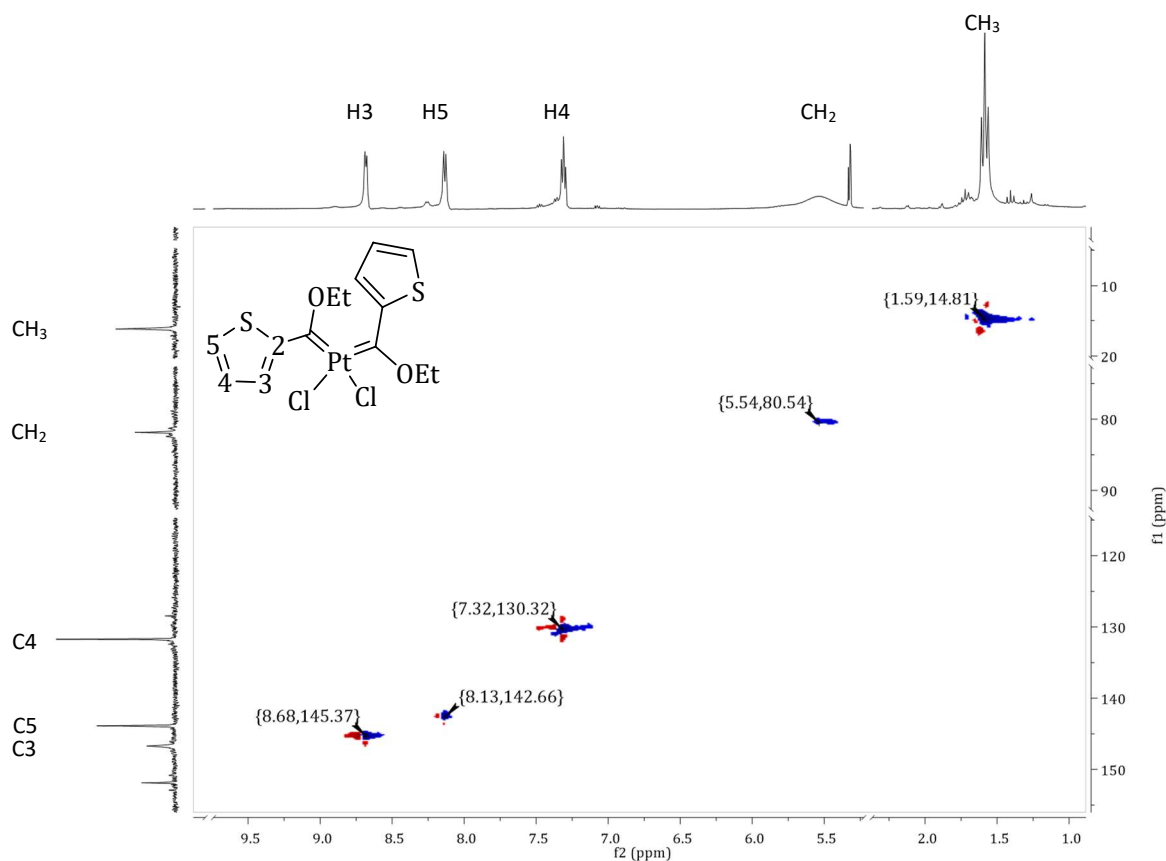


Fig. S15 2D $[^1\text{H}, ^{13}\text{C}]$ HSQC spectrum of **1**

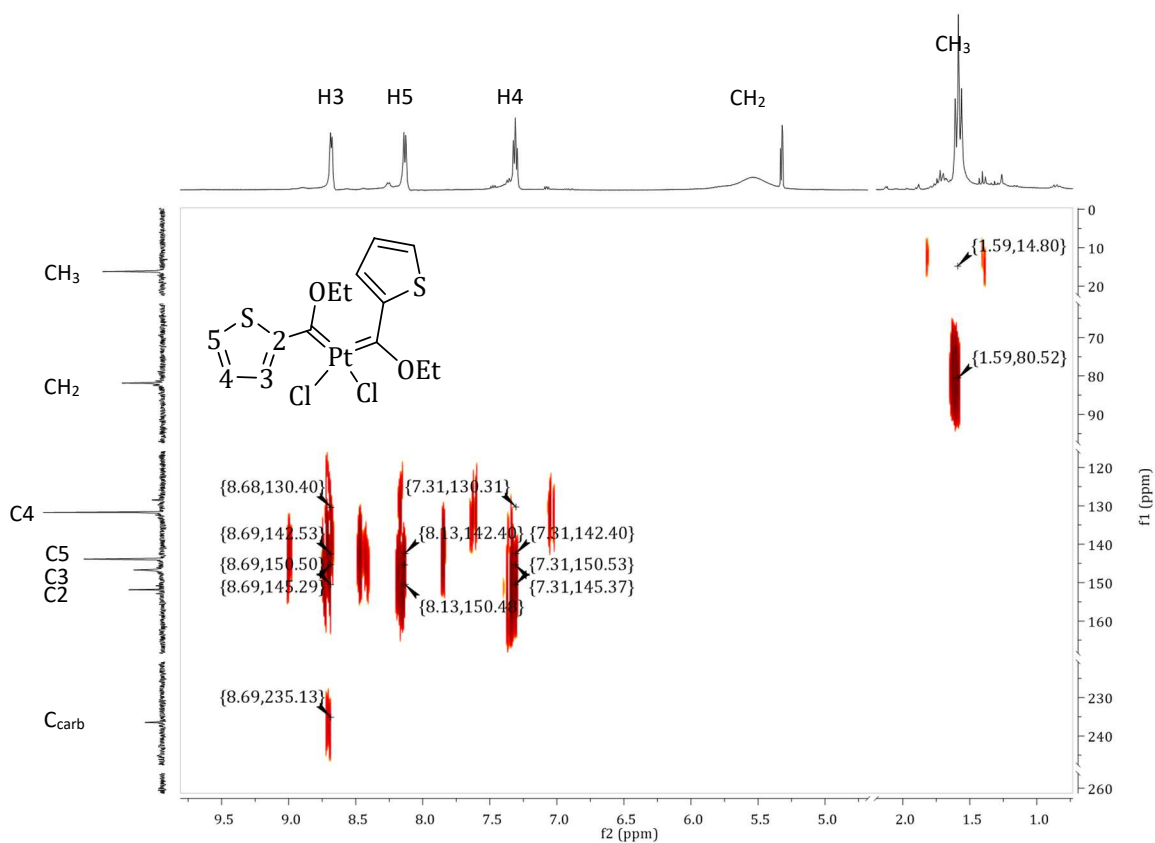


Fig. S16 2D [^1H , ^{13}C] HMBC spectrum of **1**

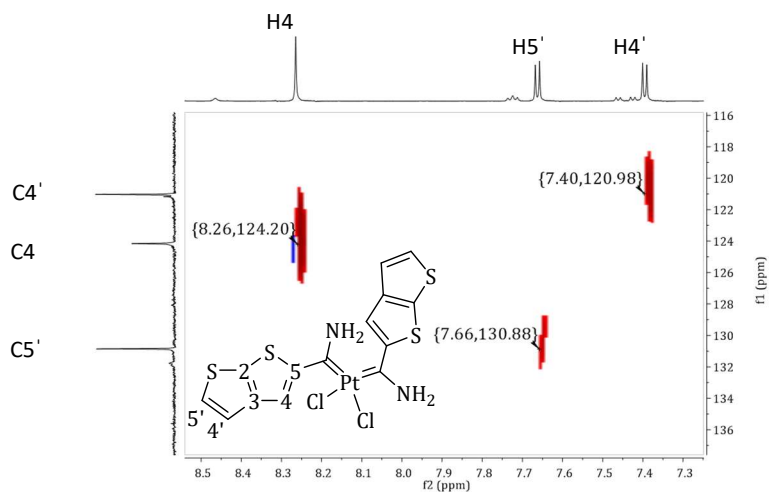


Fig. S17 2D [^1H , ^{13}C] HSQC spectrum of **3a**

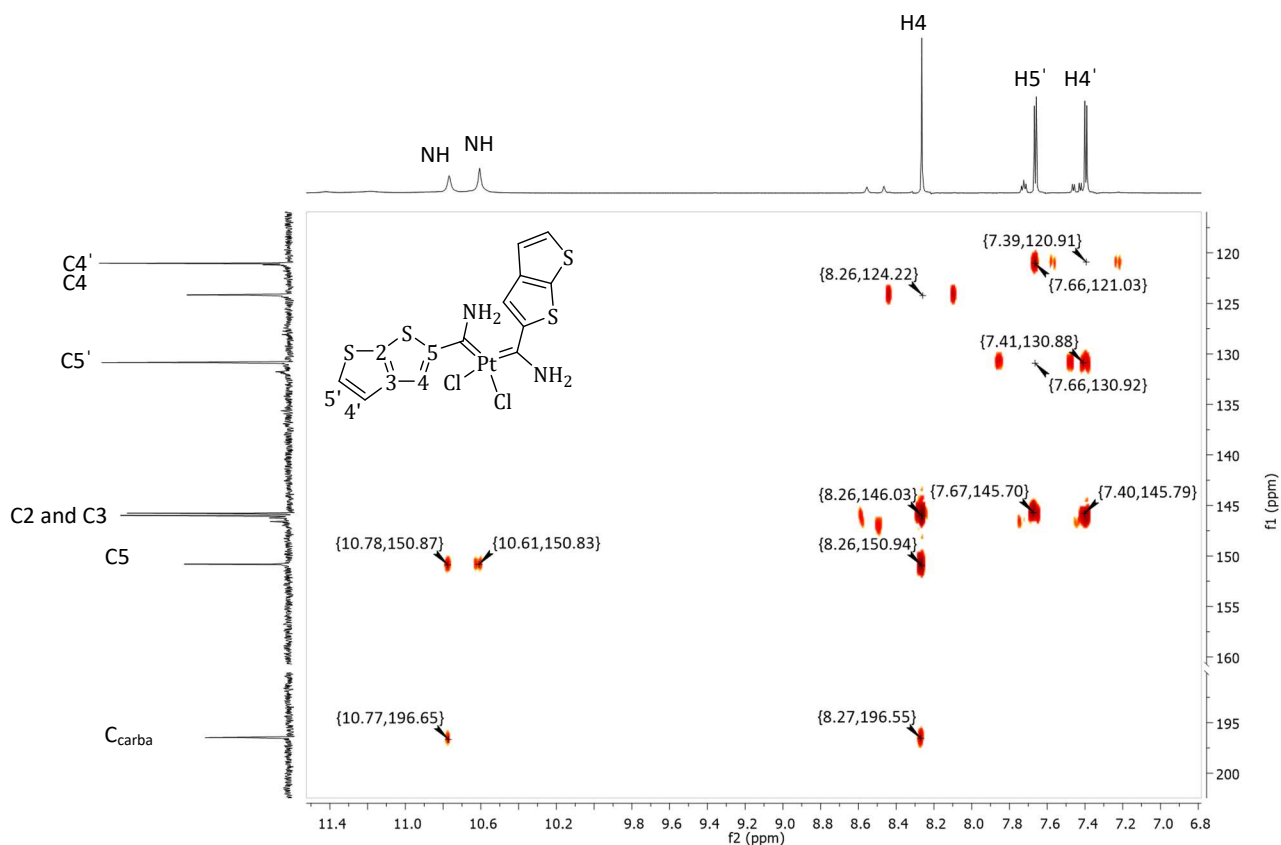


Fig. S18 2D [^1H , ^{13}C] HMBC spectrum of **3a**

S4. Molecular structures, crystal data collection and structure refinement parameters

Crystallization of **P4_w**, **2** and **5** was carried out from saturated DCM solutions of the compounds, layered with hexane. Single crystal X-ray diffraction studies confirmed the compounds' molecular structures (Fig. S19). Selected bond lengths, angles and torsion angles are reported in Table S6. The poor quality dataset of **2** as well as the observation of high electron density near the strongly absorbing platinum atoms are most likely due to strong diffuse scattering of the crystal sample.

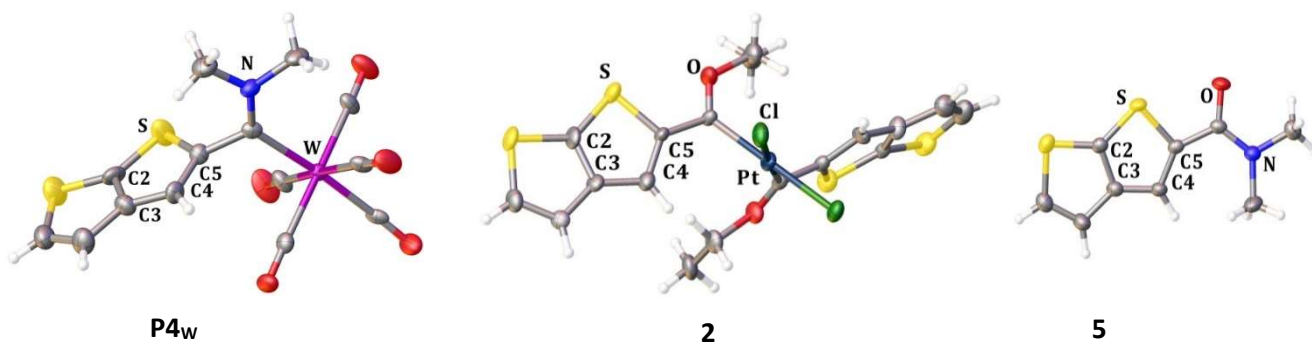


Fig. S19 The molecular structures of **P4_w**, **2** and **5** with the atomic displacement ellipsoids shown at the 50% probability level.

Compound P4w: $C_{14}H_9NO_5S_2W$ ($M = 519.19$ g/mol): triclinic, space group P-1 (no. 2), $a = 6.5766(10)$ Å, $b = 14.830(2)$ Å, $c = 17.779(3)$ Å, $\alpha = 103.000(8)^\circ$, $\beta = 94.315(7)^\circ$, $\gamma = 90.165(7)^\circ$, $V = 1684.4(5)$ Å³, $Z = 4$, $T = 150(2)$ K, $\mu(\text{MoK}\alpha) = 7.127$ mm⁻¹, $D_{\text{calc}} = 2.047$ g/cm³, 38129 reflections measured ($4.718^\circ \leq 2\theta \leq 54.192^\circ$), 6996 unique ($R_{\text{int}} = 0.0976$, $R_{\text{sigma}} = 0.0826$) which were used in all calculations. The final R_1 was 0.0537 ($I > 2\sigma(I)$) and wR_2 was 0.1241 (all data). CSD deposition number 2061164.

Compound 1: $C_{14}H_{16}Cl_2O_2PtS_2$ ($M = 546.38$ g/mol): monoclinic, space group $P2_1/n$ (no. 14), $a = 11.5072(5)$ Å, $b = 9.7623(3)$ Å, $c = 16.4968(6)$ Å, $\beta = 109.328(4)^\circ$, $V = 1748.75(12)$ Å³, $Z = 4$, $T = 150(2)$ K, $\mu(\text{MoK}\alpha) = 8.567$ mm⁻¹, $D_{\text{calc}} = 2.075$ g/cm³, 25945 reflections measured ($4.926^\circ \leq 2\theta \leq 52.738^\circ$), 3568 unique ($R_{\text{int}} = 0.0890$, $R_{\text{sigma}} = 0.0493$) which were used in all calculations. The final R_1 was 0.0453 ($I > 2\sigma(I)$) and wR_2 was 0.1105 (all data). CSD deposition number 2061166.

Compound 2: $C_{18}H_{16}Cl_2O_2PtS_4$ ($M = 658.54$ g/mol): triclinic, space group P-1 (no. 2), $a = 8.7795(10)$ Å, $b = 10.6638(11)$ Å, $c = 11.6995(13)$ Å, $\alpha = 82.207(4)^\circ$, $\beta = 75.761(4)^\circ$, $\gamma = 79.045(4)^\circ$, $V = 1037.8(2)$ Å³, $Z = 2$, $T = 150(2)$ K, $\mu(\text{MoK}\alpha) = 7.432$ mm⁻¹, $D_{\text{calc}} = 2.107$ g/cm³, 17238 reflections measured ($4.852^\circ \leq 2\theta \leq 52.708^\circ$), 4229 unique ($R_{\text{int}} = 0.0800$, $R_{\text{sigma}} = 0.0807$) which were used in all calculations. The final R_1 was 0.0722 ($I > 2\sigma(I)$) and wR_2 was 0.1668 (all data). CSD deposition number 2061163.

Compound 3b: $C_{11}H_{13}ClNOPt_{0.5}S_2$ ($M = 372.34$ g/mol): triclinic, space group P-1 (no. 2), $a = 6.9280(10)$ Å, $b = 13.774(2)$ Å, $c = 15.184(3)$ Å, $\alpha = 100.047(5)^\circ$, $\beta = 96.161(5)^\circ$, $\gamma = 90.884(5)^\circ$, $V = 1417.6(4)$ Å³, $Z = 4$, $T = 150(2)$ K, $\mu(\text{MoK}\alpha) = 5.454$ mm⁻¹, $D_{\text{calc}} = 1.745$ g/cm³, 44056 reflections measured ($4.412^\circ \leq 2\theta \leq 52.74^\circ$), 5801 unique ($R_{\text{int}} = 0.0478$, $R_{\text{sigma}} = 0.0261$) which were used in all calculations. The final R_1 was 0.0181 ($I > 2\sigma(I)$) and wR_2 was 0.0469 (all data). CSD deposition number 2061167.

Compound 4a: $C_{18}H_{18}Cl_2N_2PtS_4$ ($M = 656.57$ g/mol): monoclinic, space group $P2_1/c$ (no. 14), $a = 11.1318(6)$ Å, $b = 17.0266(7)$ Å, $c = 12.4532(7)$ Å, $\beta = 110.318(7)^\circ$, $V = 2213.5(2)$ Å³, $Z = 4$, $T = 293(2)$ K, $\mu(\text{MoK}\alpha) = 6.965$ mm⁻¹, $D_{\text{calc}} = 1.970$ g/cm³, 29159 reflections measured ($3.902^\circ \leq 2\theta \leq 52.742^\circ$), 4528 unique ($R_{\text{int}} = 0.2114$, $R_{\text{sigma}} = 0.1233$) which were used in all calculations. The final R_1 was 0.0554 ($I > 2\sigma(I)$) and wR_2 was 0.1327 (all data). CSD deposition number 2061165.

Compound 5: $C_9H_9NOS_2$ ($M = 211.29$ g/mol): monoclinic, space group $P2_1/c$ (no. 14), $a = 27.501(2)$ Å, $b = 5.8805(4)$ Å, $c = 11.7976(8)$ Å, $\beta = 97.085(4)^\circ$, $V = 1893.4(2)$ Å³, $Z = 8$, $T = 150(2)$ K, $\mu(\text{CuK}\alpha) = 4.746$ mm⁻¹, $D_{\text{calc}} = 1.482$ g/cm³, 55462 reflections measured ($6.478^\circ \leq 2\theta \leq 144.214^\circ$), 3734 unique ($R_{\text{int}} = 0.1301$, $R_{\text{sigma}} = 0.0381$) which were used in all calculations. The final R_1 was 0.0408 ($I > 2\sigma(I)$) and wR_2 was 0.1117 (all data). CSD deposition number 2061168.

Table S6 Selected bond lengths (Å) and angles (°) of **P4_w** and **5**

Complex	P4_w	5^c
Bond lengths		
M/O—C _{carb}	2.26(1)	1.243(3)
C _{carb} —N	1.31(1)	1.345(4)
M—CO <i>trans to CO^a</i>	2.04(1)	
M—CO <i>trans to C_{carb}</i>	2.03(1)	
C _{carb} —C2/C5	1.48(1)	1.482(3)
C2—C3	1.37(2)	1.381(3)
C3—C4	1.47(1)	1.421(3)
C4—C5	1.36(2)	1.366(3)
S—C2	1.73(1)	1.716(2)
S—C5	1.76(1)	1.749(3)
Bond angles		
M/O—C _{carb} —N	129.3(7)	121.2(2)
M/O—C _{carb} —C2/C5	116.0(7)	117.5(2)
N—C _{carb} —C2/C5	114.7(9)	121.3(2)
Torsion angles		
M/O—C _{carb} — C2/C5—C3/C4	-91(1)	162.9(3)
N—C _{carb} — C2/C5—C3/C4	87(1)	-17.9(4)
Angle between two mean planes^b	89.01	15.53

^a Averaged bond length.

^b First mean plane drawn through C2, C3, C4 and C5, and the second through M/O, C_{carb} and N.

^c Compound **5** does not have a C_{carb} but a quaternary carbon, as the metal fragment is replaced by O.

S5. Crystal packing.

Inter- and intramolecular hydrogen bonding interactions are possible in **3b** and **5** and are illustrated in Fig. S20. Only the interactions closer than 2.6 Å are reported. The intermolecular hydrogen bonding interactions are abundant and occur between H···O/Cl. Intramolecular hydrogen bonding interactions are more rare and only one is observed in **3b** and two in **5** (interaction distance reported in green, Fig. S20). In the case of **3b** the interaction is between NH···S (2.561 Å) and in **5** between NCH···O (2.419 and 2.238 Å).

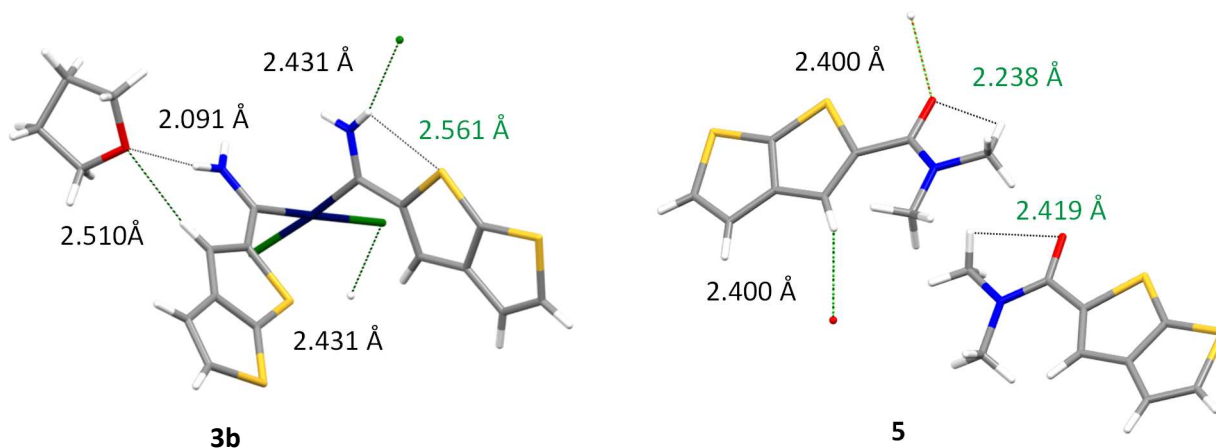


Fig. S20. Inter- and intramolecular hydrogen bonding interactions observed in the solid state structures of **3b** and **5**

The duplication of resonances in the ^1H NMR spectrum of **3b** indicates two different carbene fragments in the molecule (Fig. S9, *vide supra*). As the molecule is symmetric the duplication of proton resonances is the result of hydrogen bonding interactions restricting rotation in the molecule. The NH···S intramolecular interaction takes place where the sulphurs of the thienylene spacer are *cis* to the NH_2 unit and cannot take place if the sulphurs of the thienylene spacer are *trans* to the NH_2 unit. Where the sulphurs of the thienylene spacer are *trans* to the NH_2 unit, intermolecular hydrogen bonding interactions occur between TT-H4 and NH with the oxygen of a co-crystallized THF molecule (2.510 and 2.091 Å, respectively). Thus, two different orientated TT spacers are observed.

In the crystal packing of **3b**, π - π stacking of both the [2,3-*b*]-TT spacers take place. Their π - π interaction distances alternate between 3.331 and 3.810 Å (Fig. S21a). The molecules do not fit exactly on top of each other but the greater part of their thienylene spacers overlap. In the case of **1**, only one of the two thiophene spacers undergoes π - π stacking. Partial overlap of the thiophenes occurs with a π - π interaction distance of 3.465 Å. The π - π stacking observed for **4a** occurs between the [2,3-*b*]-TT spacers of the same molecule (partial overlap) with the π - π interaction distance measured between 3.473-3.905 Å (Fig. S21b). The neighbouring molecules are close enough to be considered π - π stacking, but as the stacking approach side on overlap it is not true π - π stacking.

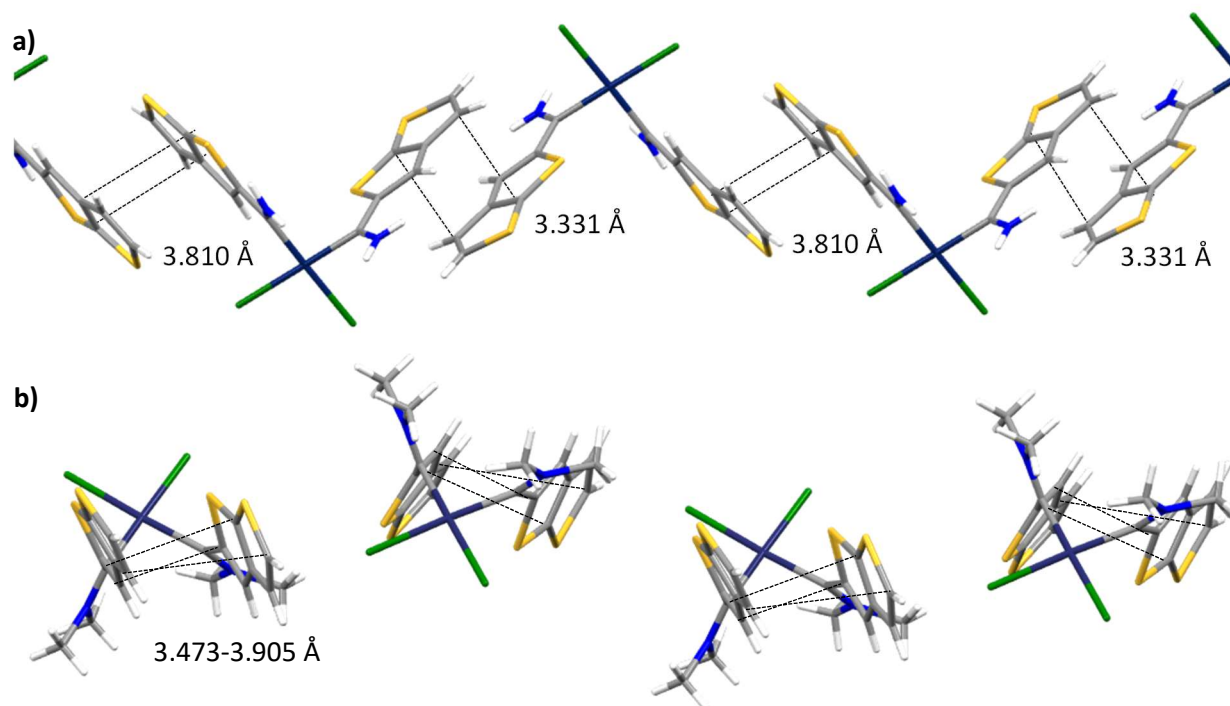


Fig. S21. Inter- and intramolecular π - π stacking of both the [2,3-b]-TT spacers of **3b** (a) and **4a** (b), respectively

S6. Hydrosilylation catalysis

Percentage conversion (conv.) is calculated as an averaged value of the conversion of both substrates, with the reactions done in duplicate. For experiments 1-15 (Table 4), complete (100% conversion) of the phenylacetylene was accompanied by unreacted triethylsilane, hence conversions from 94% and up are considered complete. Conversions are calculated as follows:

$$\text{Conv. (\%)} = \left(\frac{\text{Initial amount of substrate 1} - \text{Remaining amount of substrate 1}}{\text{Initial amount of substrate 1}} + \frac{\text{Initial amount of substrate 2} - \text{Remaining amount of substrate 2}}{\text{Initial amount of substrate 2}} \right) \div 2 \times \frac{100}{1}$$

Percentage yields are reported as an averaged value of the duplicated reactions, incorporating only the hydrosilylation isomeric products' yields and are summarized in Table 4 and 5. In the equation, the limiting substrate is usually the alkyne used in the hydrosilylation reactions. Yields are calculated as follows:

$$\text{Yield (\%)} = \left(\frac{\text{Amount of } \beta - E - \text{ isomer formed}}{\text{Initial amount of limiting substrate}} + \frac{\text{Amount of } \alpha - \text{ isomer formed}}{\text{Initial amount of limiting substrate}} + \frac{\text{Amount of } \beta - Z - \text{ isomer formed}}{\text{Initial amount of limiting substrate}} \right) \times \frac{100}{1}$$

Turnover numbers (TONs) and turnover frequencies (TOFs) are reported in Table 4 and Table 5. Again the calculated values represent an average of the duplicated reactions. TON and TOF were calculated as follows:

$$\text{TON} = \frac{\text{Mol product}}{\text{Mol catalyst}}$$
$$\text{TOF (h}^{-1}\text{)} = \frac{\text{Mol product}}{\text{Mol catalyst} \times \text{Reaction time}}$$

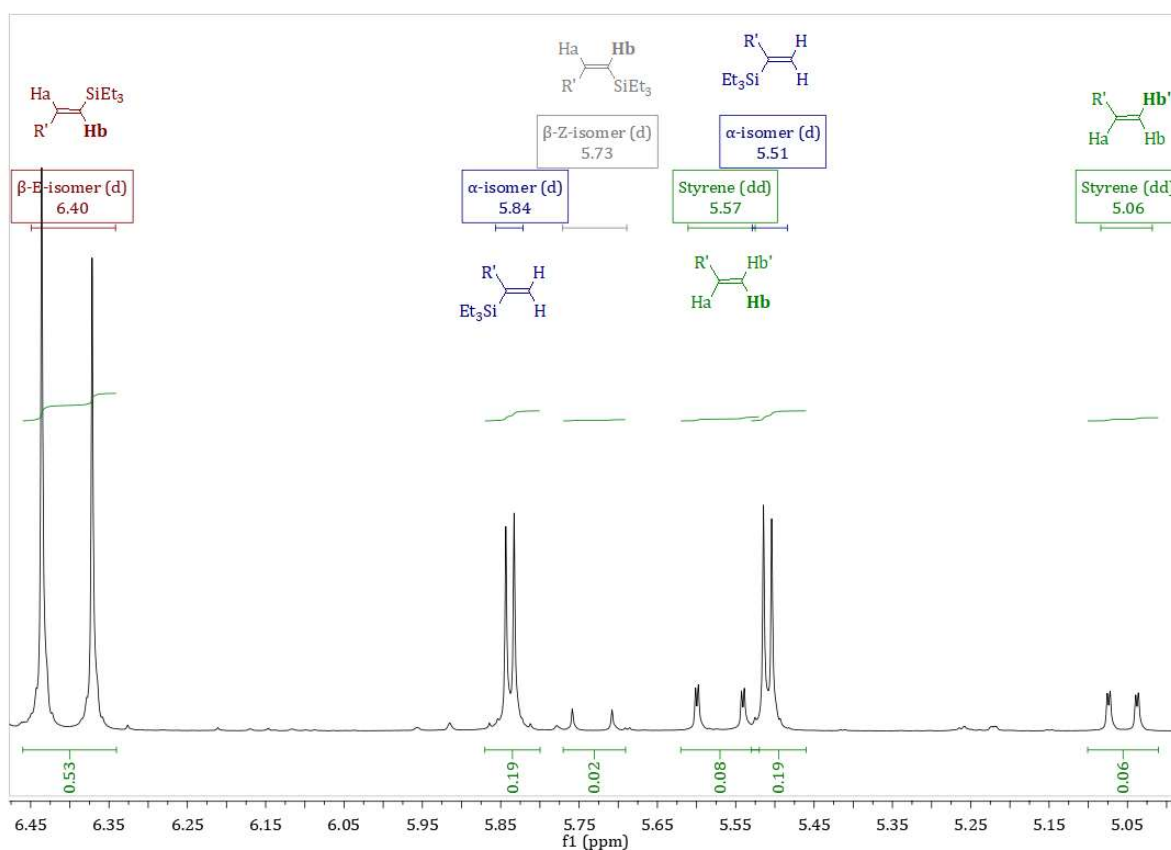


Fig. S22 ^1H NMR spectrum of entry 9, Table 4 in toluene- d_8 , in the range 5.05-6.45 ppm

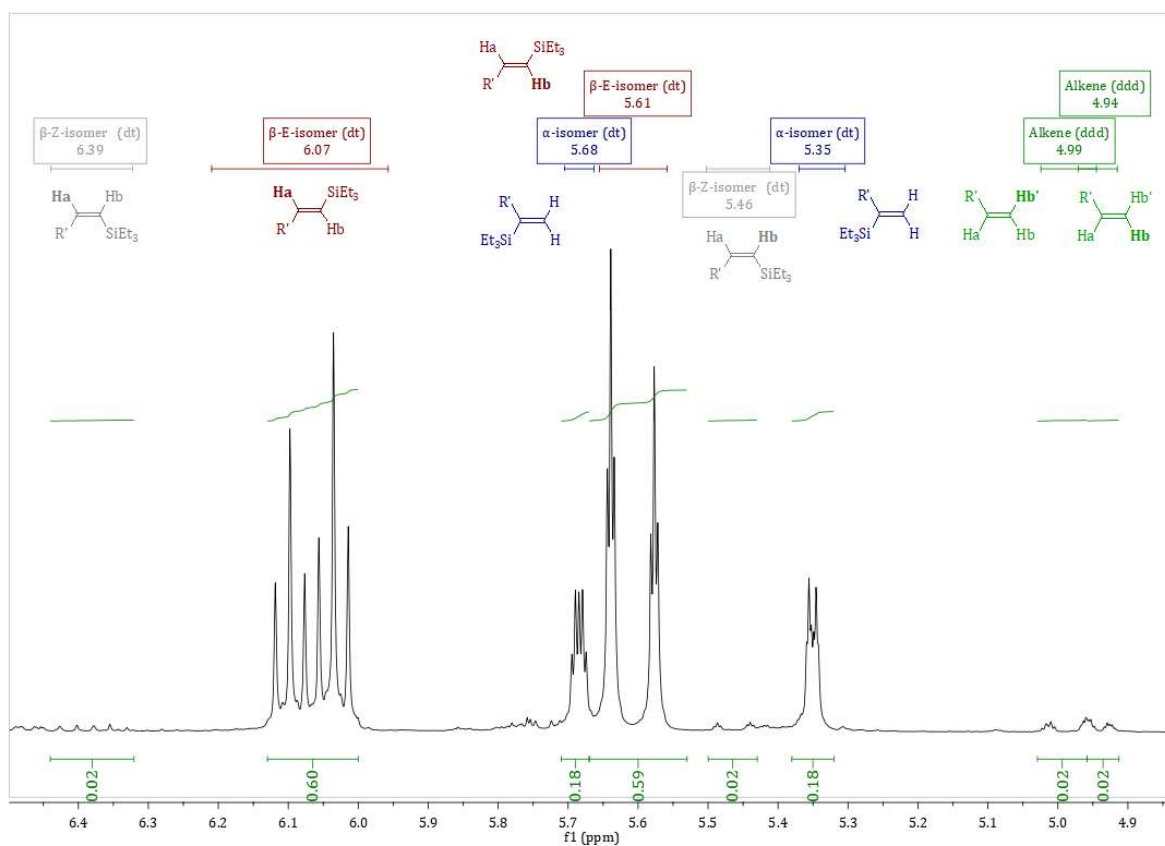


Fig. S23 ^1H NMR spectrum of entry 1, Table 5 in toluene- d_8 , in the range 4.90-6.40 ppm

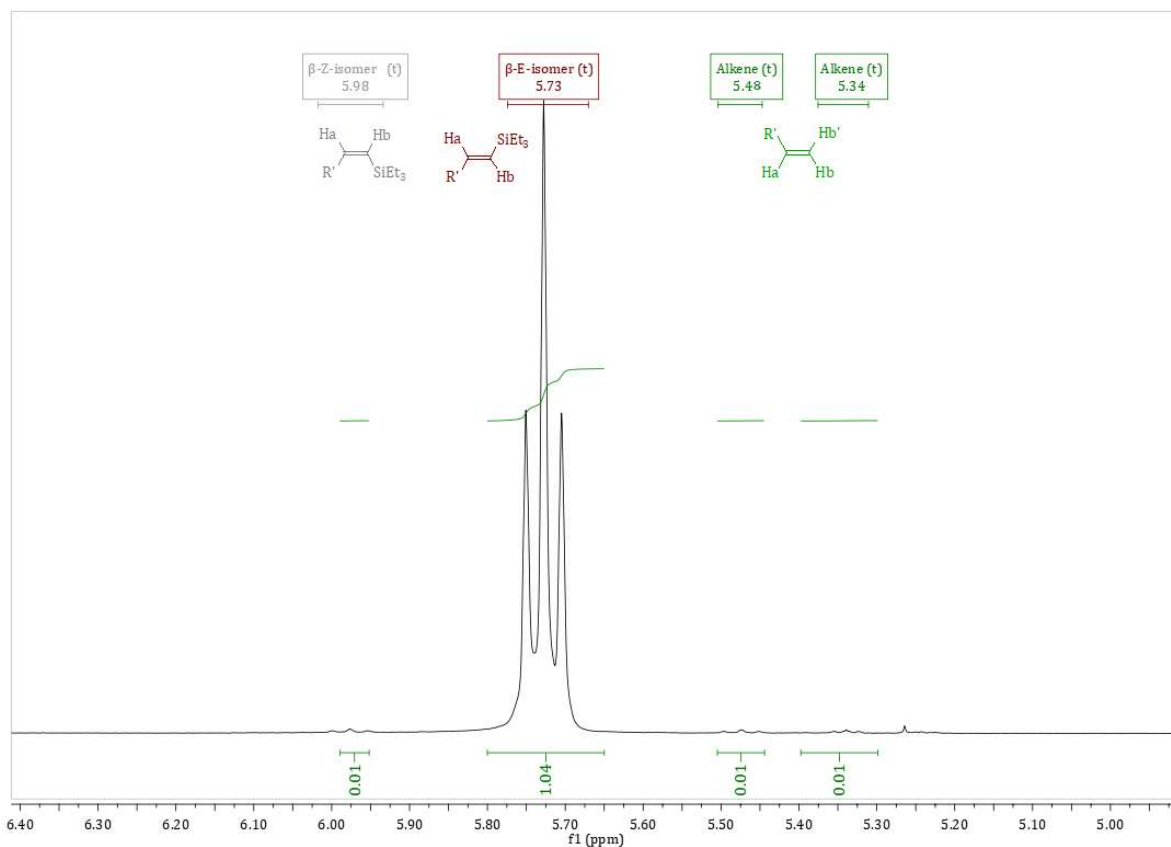


Fig. S24 ¹H NMR spectrum of entry 2, Table 5 in toluene-d₈, in the range 5.00-6.40 ppm

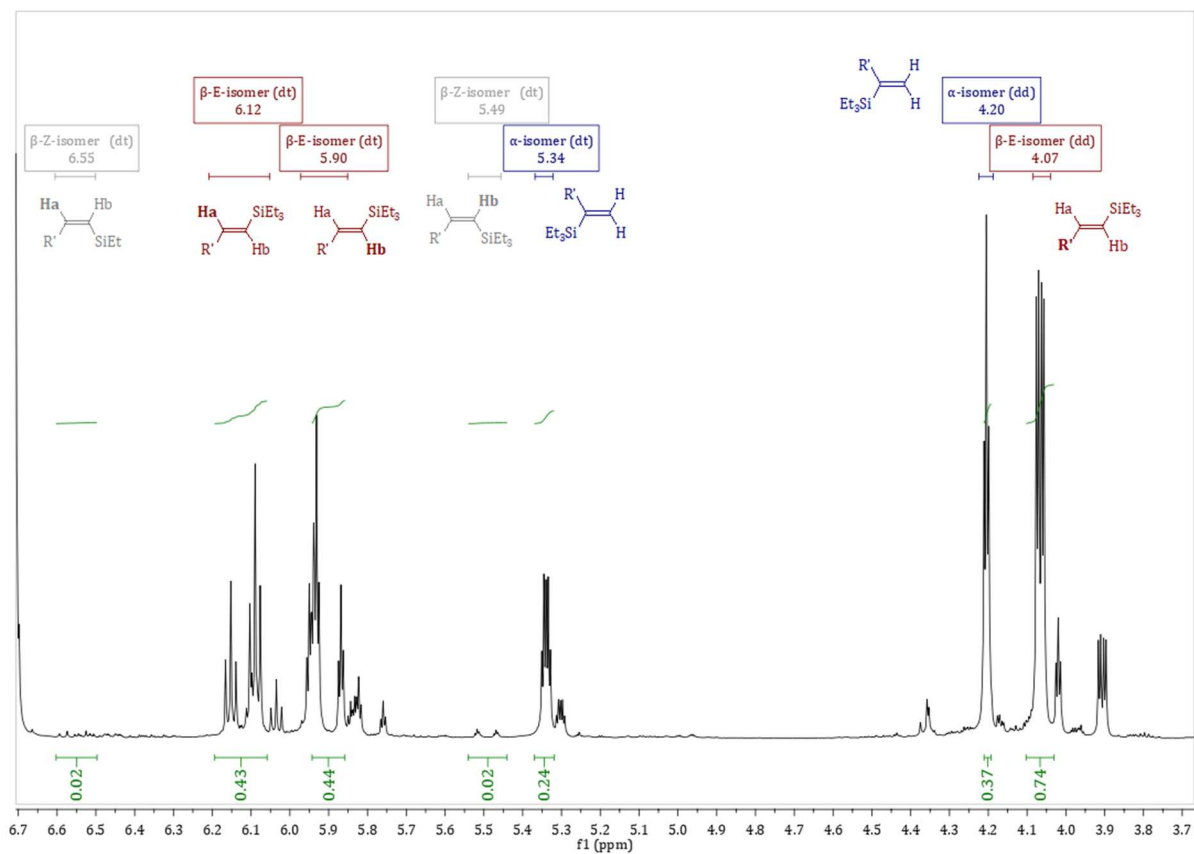


Fig. S25 ¹H NMR spectrum of entry 3, Table 5 in toluene-d₈, in the range 3.70-6.70 ppm

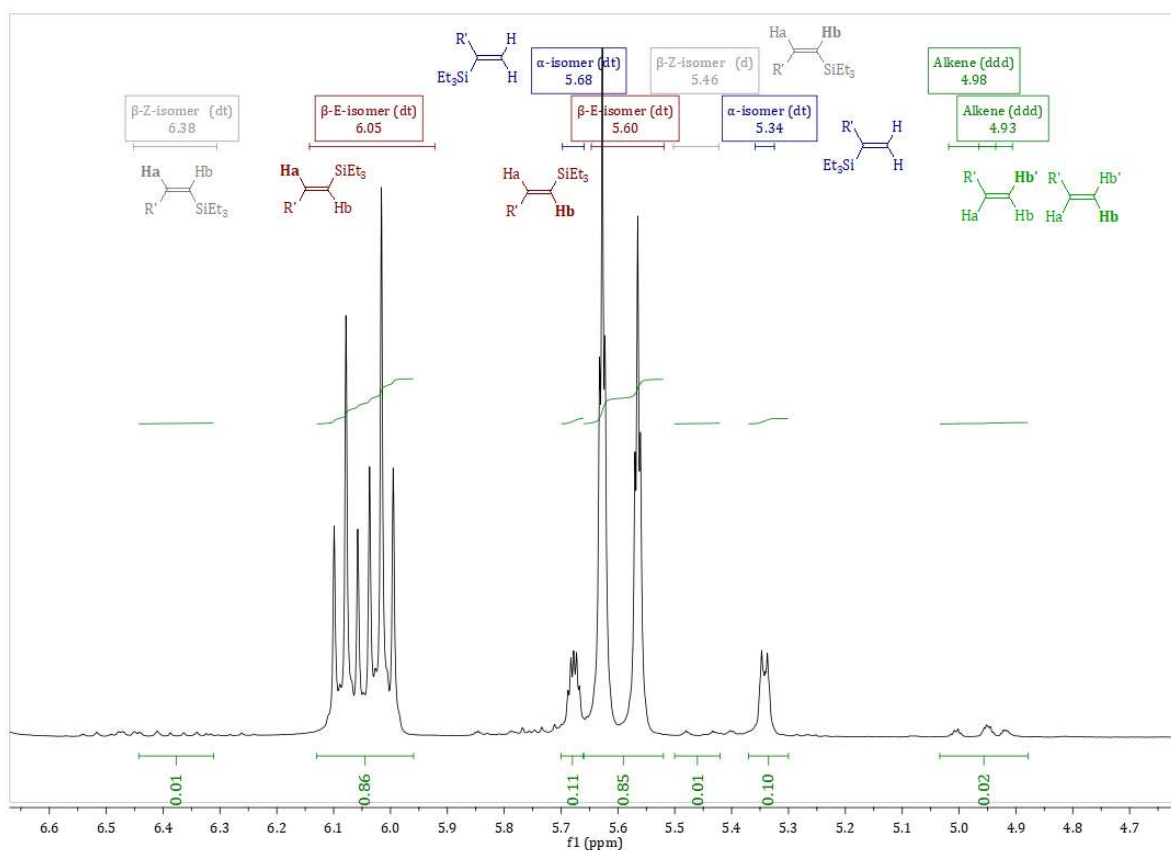


Fig. S26 ^1H NMR spectrum of entry 4, Table 5 in toluene- d_8 , in the range 4.70-6.60 ppm

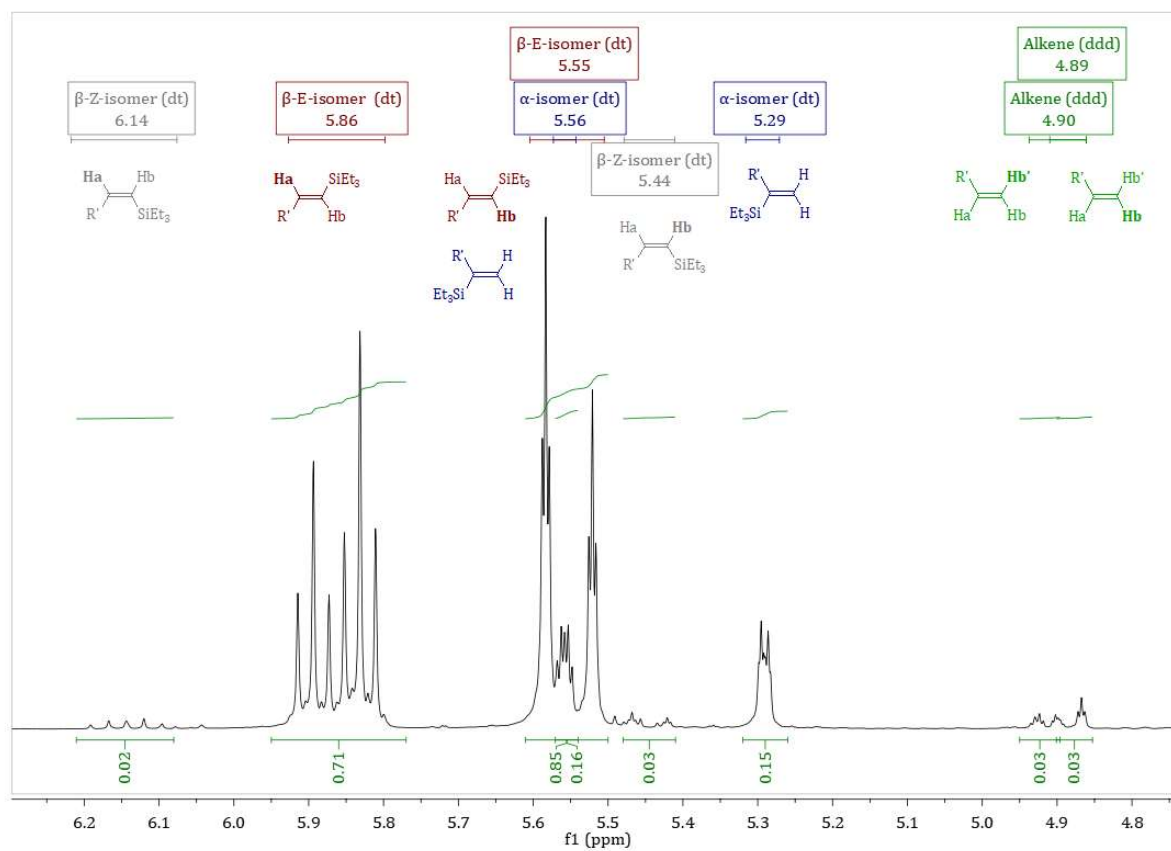


Fig. S27 ^1H NMR spectrum of entry 5, Table 5 in toluene- d_8 , in the range 4.80-6.20 ppm

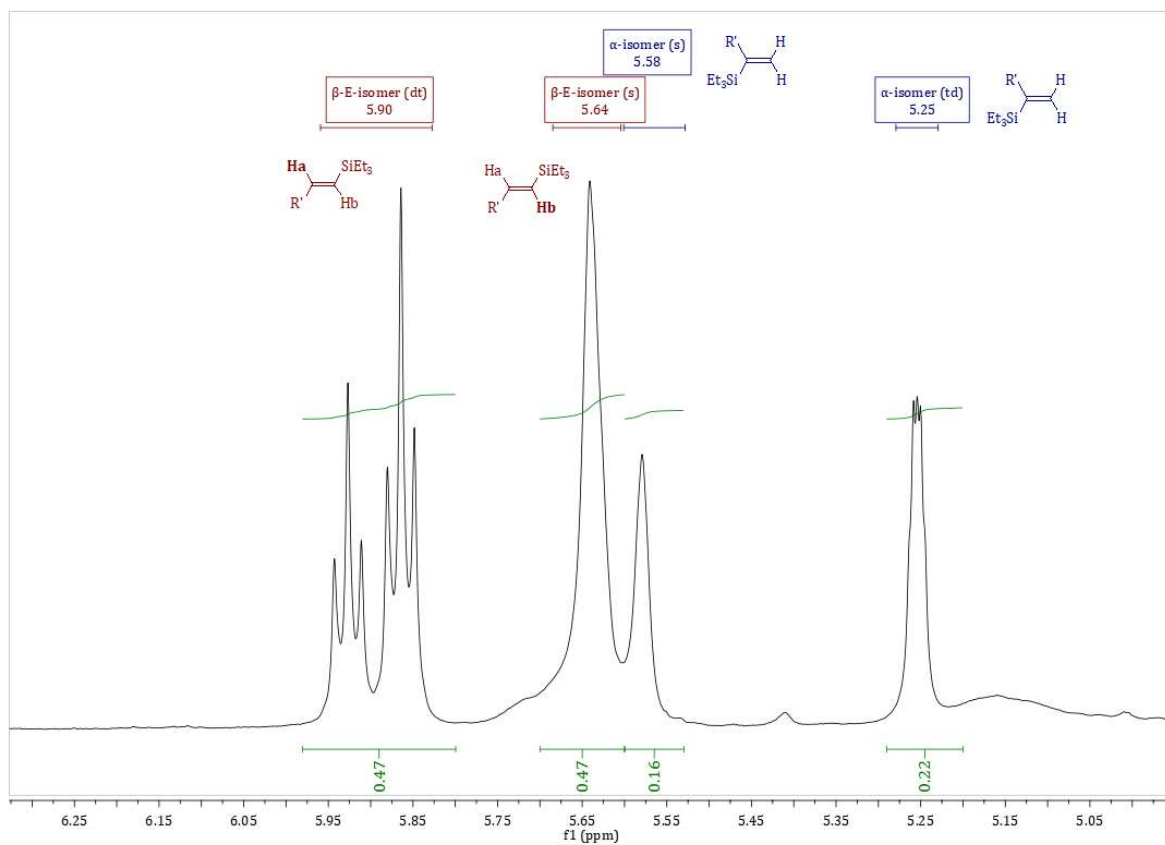
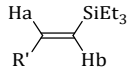
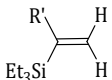
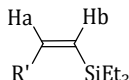
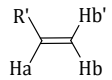
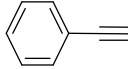
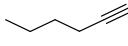
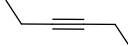
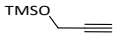
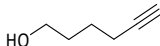
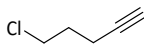
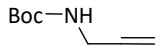


Fig. S28 ^1H NMR spectrum of entry 7, Table 5 in toluene- d_8 , in the range 5.05-6.25 ppm

Table S7 NMR data for products obtained during hydrosilylation, measured in toluene-d8 and reported in ppm (Hz)

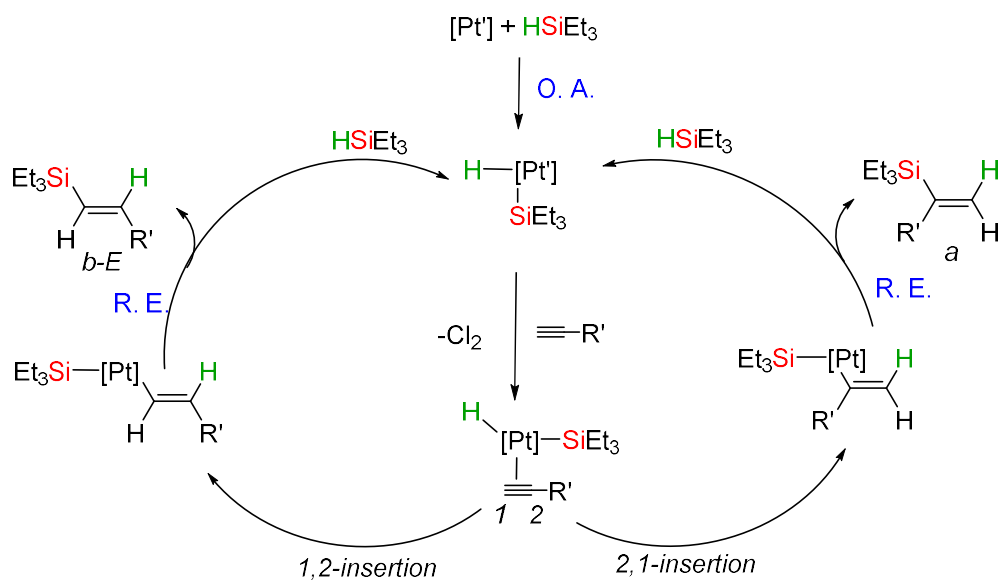
Substrate R'-≡	β -E-isomer 	α -isomer 	β -Z-isomer 	Alkene 
	6.40 (1 H, d, 3J 19.3, Hb) ⁴	5.84 (1 H, d, 2J 3.2), 5.51 (1 H, d, 2J 3.2) ⁵	5.73 (1 H, d, 3J 15.2, Hb) ⁶	5.57 (1 H, dd, 3J 17.6, 2J 1.0, Hb), 5.06 (1 H, dd, 3J 10.9, 2J 1.0, Hb') ⁷
	6.07 (1 H, dt, 3J 18.7 and 6.29, Ha), 5.61 (1 H, dt, 3J 18.7, 4J 1.5, Hb) ⁸	5.68 (1 H, dt, 2J 3.1, 4J 1.6), 5.35 (1 H, dt, 2J 3.0, 4J 0.9) ⁸	6.39 (1 H, dt, 3J 14.3 and 7.2, Ha), 5.46 (1 H, dt, 3J 14.2, 4J 1.4, Hb) ^{9,10}	4.99 (1 H, ddd, J 17.1, 2.2, 1.6, Hb'), 4.94 (1 H, ddd, J 4.6, 2.2, 1.0, Hb) ¹¹
	5.73 (1 H, t, 3J 6.9) ^{12,13}	-	5.98 (1 H, t, 3J 6.9)	5.48 (2 H, t, 3J 6.8, E-isomer), 5.34 (2 H, t, 3J 5.1, Z-isomer) ^{14,15}
	6.12 (1 H, dt, 3J 18.8 and 4.0, Ha), 5.90 (1 H, dt, 3J 18.8, 2J 1.8, Hb), 4.07 (2 H, dd, 3J 4.0, 2J 1.8, R') ^{16a}	5.34 (1 H, dt, 2J 3.3, 4J 1.7), 4.20 (1 H, dd, 4J 1.8) ^a	6.55 (1 H, dt, 3J 14.6 and 5.9, Ha), 5.49 (1 H, dt, 3J 14.6, 4J 1.5, Hb) ¹⁶	-
	6.05 (1 H, dt, 3J 18.7 and 6.3, Ha), 5.60 (1 H, dt, 3J 18.7, 2J 1.4, Hb)	5.68 (1 H, dt, 2J 3.0, 4J 1.5), 5.34 (1 H, dt, 2J 3.1, 4J 1.0)	6.38 (1 H, dt, 3J 14.4 and 8.0, Ha), 5.46 (1 H, dt, 3J 14.2, 4J 1.2, Hb) ⁹	4.98 (1 H, ddd, J 17.1, 2.4, 1.6, Hb'), 4.93 (1 H, ddd, J 4.5, 2.2, 1.1, Hb)
	5.86 (1 H, dt, 3J 18.7 and 6.3, Ha), 5.55 (1 H, dt, 3J 18.7, 2J 1.4, Hb) ¹⁷	5.56 (1 H, dt, 2J 2.9, 4J 1.5), 5.29 (1 H, dt, 2J 2.6, 4J 0.9)	6.14 (1 H, dt, 3J 14.3 and 7.3, Ha), 5.44 (1 H, dt, 3J 14.1, 4J 1.3, Hb) ¹⁷	4.90 (1 H, ddd, J 16.6, 2.3, 1.5, Hb'), 4.89 (1 H, ddd, J 8.7, 2.5, 1.3, Hb)
	5.90 (1 H, dt, 3J 18.8 and 4.8, Ha), 5.64 (1 H, s, br, Hb)	5.58 (1 H, s, br), 5.25 (1 H, dt, 2J 2.6, 4J 1.4)	-	4.52 (br), 4.43 (br)

^a Resonances are exactly duplicated upfield in smaller variations.

Table S8 Reaction conditions for the specific catalytic reactions

Entry	Catalyst	Catalyst loading (mol%)	Alkyne (0.25 mmol, μ L)	Time (hrs)	Byproducts (% yield)
1 ^a (Table 4)	2	2	-	6	-
2 ^a (Table 4)	-	-	Phenylacetylene (27.5)	6	Styrene (1)
3 (Table 4)	2	1	Phenylacetylene (27.5)	6	Styrene (6), triethyl-(phenylethynyl)silane (<1)
4 (Table 4)	2	0.5	Phenylacetylene (27.5)	6	Styrene (6), triethyl-(phenylethynyl)silane (<1)
5 (Table 4)	2	0.3	Phenylacetylene (27.5)	6	Styrene (7), triethyl-(phenylethynyl)silane (<1)
6 (Table 4)	2	0.2	Phenylacetylene (27.5)	6	Styrene (2), triethyl-(phenylethynyl)silane (<1)
7 (Table 4)	2	0.3	Phenylacetylene (27.5)	6	Styrene (1), triethyl-(phenylethynyl)silane (<1)
8 (Table 4)	2	0.3	Phenylacetylene (27.5)	3	Styrene (6), triethyl-(phenylethynyl)silane (<1)
9 (Table 4)	2	0.3	Phenylacetylene (27.5)	2	Styrene (6), triethyl-(phenylethynyl)silane (<1)
10 (Table 4)	2	0.3	Phenylacetylene (27.5)	1	Styrene (3), triethyl-(phenylethynyl)silane (<1)
11 (Table 4)	1	0.3	Phenylacetylene (27.5)	2	Styrene (6), triethyl-(phenylethynyl)silane (2)
12 (Table 4)	K_2PtCl_4	0.3	Phenylacetylene (27.5)	2	-
13 (Table 4)	<i>cis</i> -[PtCl ₂ (NCMe) ₂]	0.3	Phenylacetylene (27.5)	2	Styrene (2), triethyl-(phenylethynyl)silane (<1)
14 ^b (Table 4)	2	0.3	Phenylacetylene (27.5)	2	-
15 ^b (Table 4)	1	0.3	Phenylacetylene (27.5)	2	-
1 (Table 5)	2	0.3	1-Hexyne (28.5)	2	Alkene (2)
2 (Table 5)	2	0.3	3-Hexyne (28.5)	2	<i>E</i> -Alkene (1), <i>Z</i> -Alkene (0)
3 (Table 5)	2	0.3	3-TMSO-1-propyne (37.5)	2	-
4 (Table 5)	2	0.3	5-Hexyn-1-ol (27.5)	2	Alkene (1)
5 (Table 5)	2	0.3	5-Chloro-1-pentyn (26.5)	2	Alkene (3)
6 (Table 5)	2	0.3	Propargylamine (16.0)	2	-
7 (Table 5)	2	0.3	N-Boc-propargylamine (38.8)	2	Alkene (22)
8 (Table 5)	2	0.3	Bis(trimethylsilyl)acetylene (55.0)	2	-
9 (Table 5)	2	0.3	1-Hexyne (28.5)	1	Alkene (2)
10 (Table 5)	2	0.3	3-Hexyne (28.5)	1	<i>E</i> -Alkene (1), <i>Z</i> -Alkene (0)
11 (Table 5)	2	0.3	N-Boc-propargylamine (38.8)	1	Alkene (15)
12 (Table 5)	2	0.3	5-Hexyn-1-ol (27.5)	1	Alkene (2)

^a Experiments not performed in duplicate.^b Reactions done neat



O. A. = oxidative addition

R. E. = reductive elimination

[Pt'] = *cis*-[PtCl₂{C(OEt)-2-C₄H₃S₂}₂] (**1**), *cis*-[PtCl₂{C(OEt)-5-C₆H₃S₂}₂] (**2**)

[Pt] = *cis*-[Pt{C(OEt)-2-C₄H₃S₂}₂] (**1**), *cis*-[Pt{C(OEt)-5-C₆H₃S₂}₂] (**2**)

Scheme S2. Proposed mechanistic cycle for the standard Chalk-Harrod mechanism of **1**- and **2**-catalyzed alkyne hydrosilylation

S7. ESI-MS

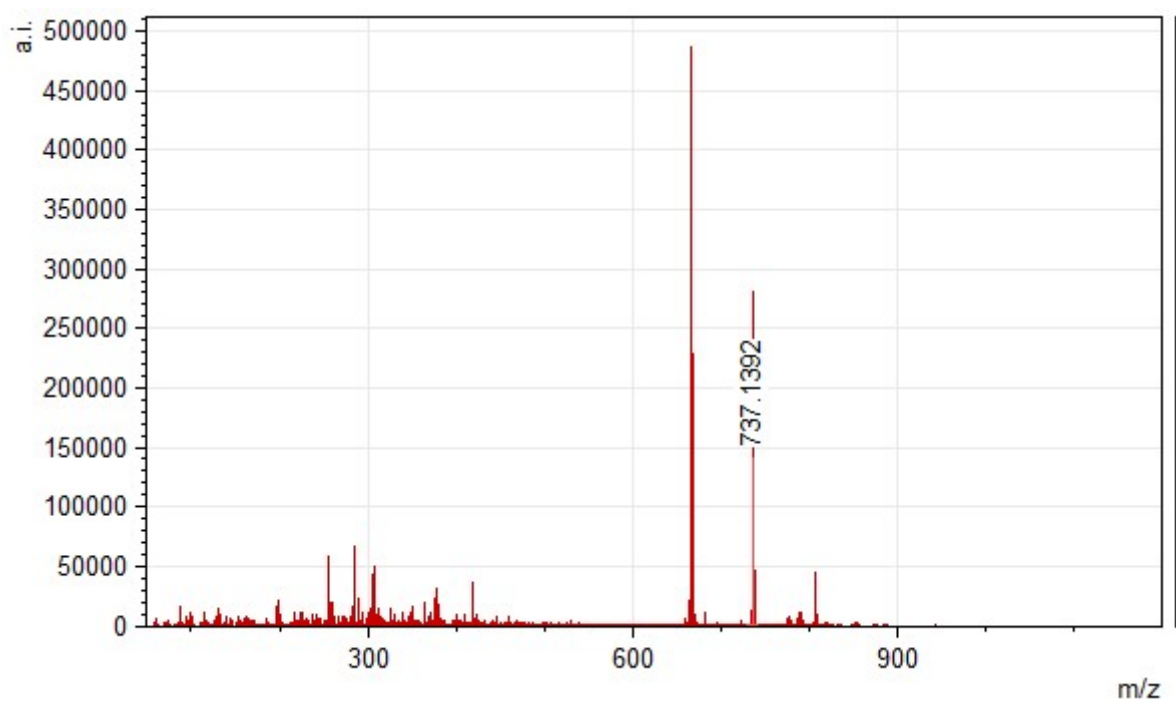


Fig. S29 ESI-MS of compound 1.

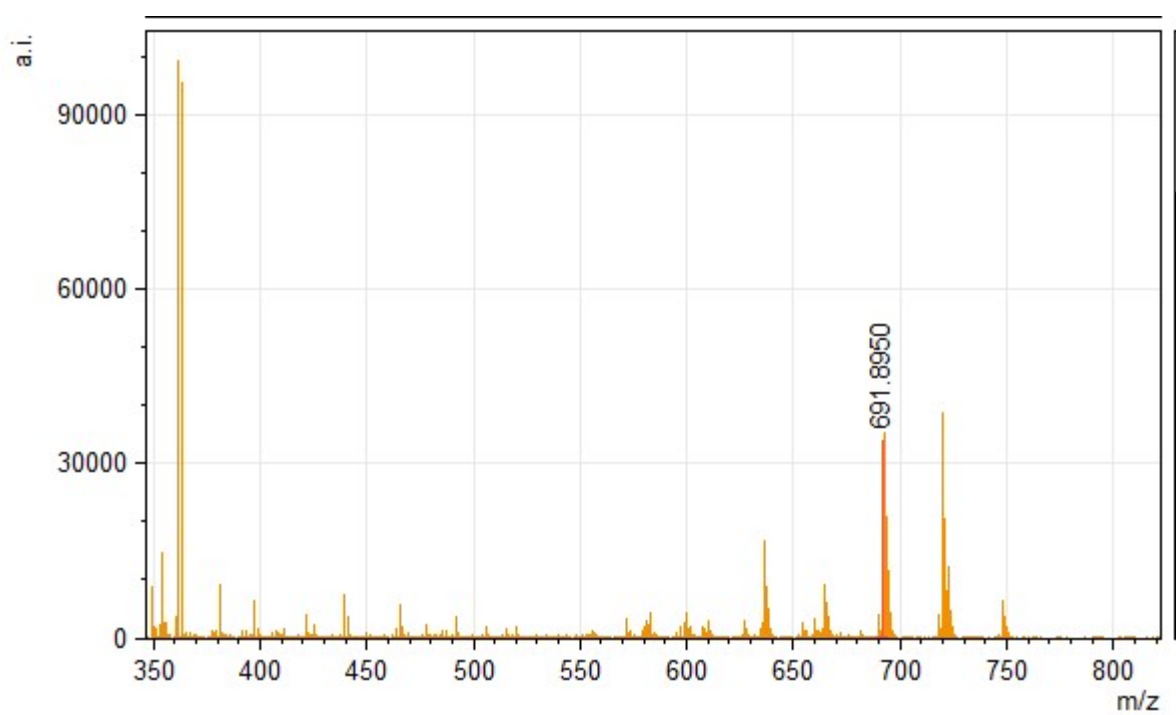


Fig. S30 ESI-MS of compound 2.

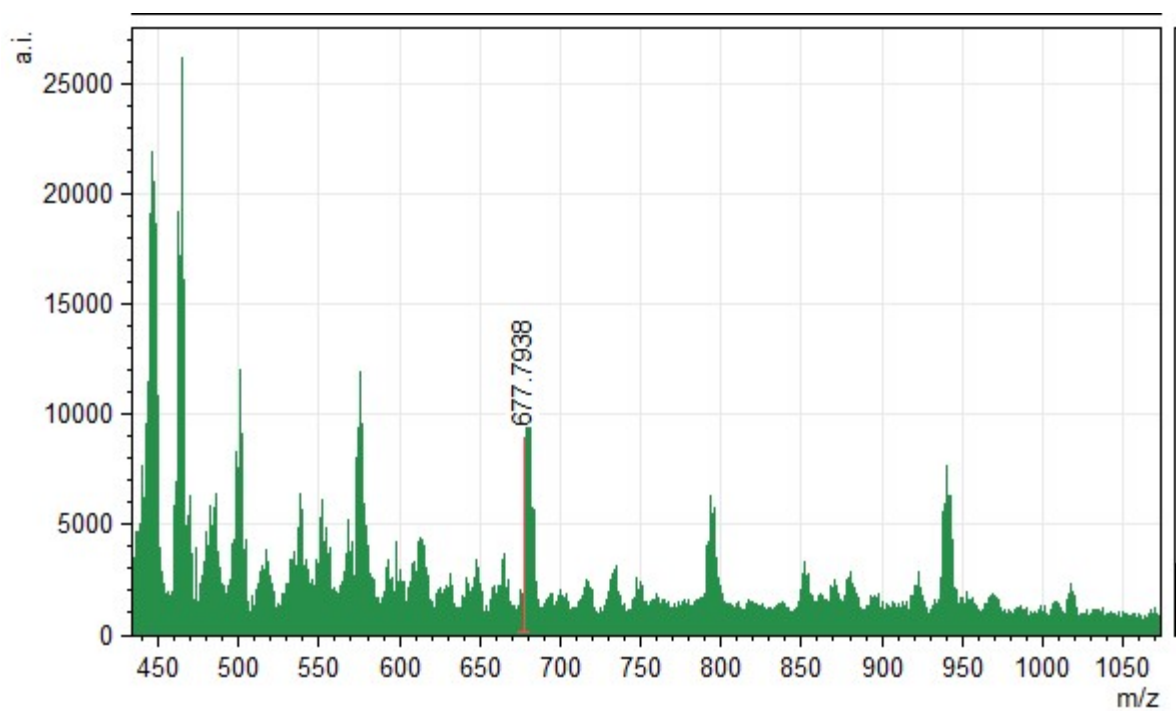


Fig. S31 ESI-MS of compound **3a**.

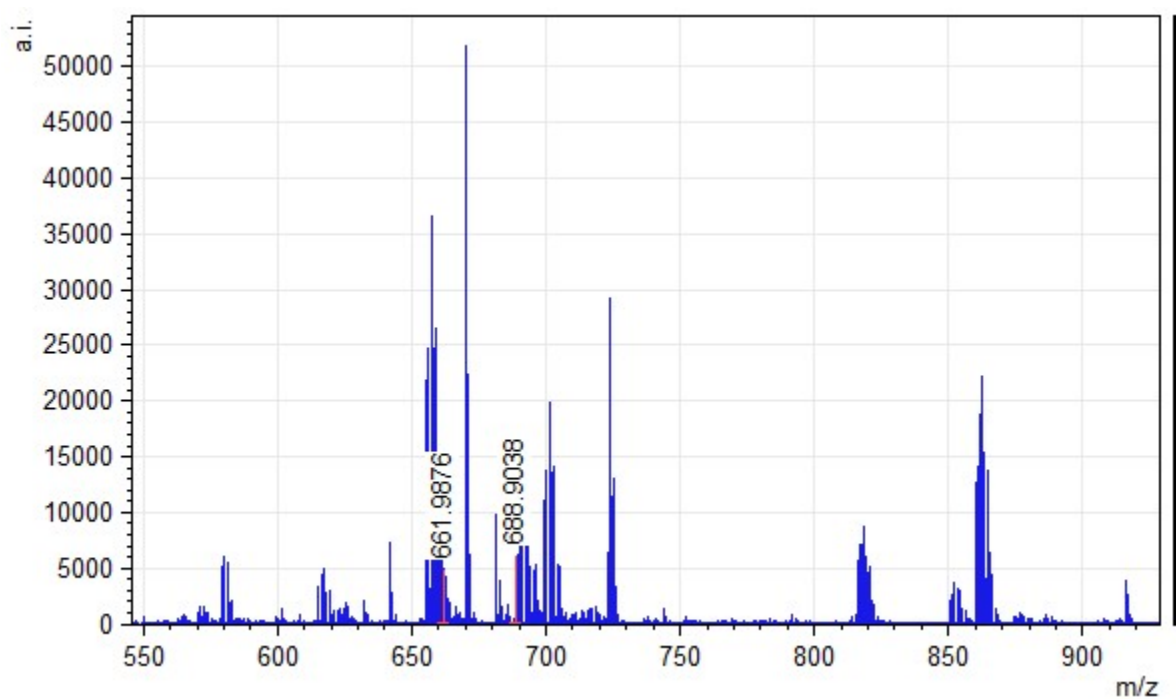


Fig. S32 ESI-MS of compound **4a**

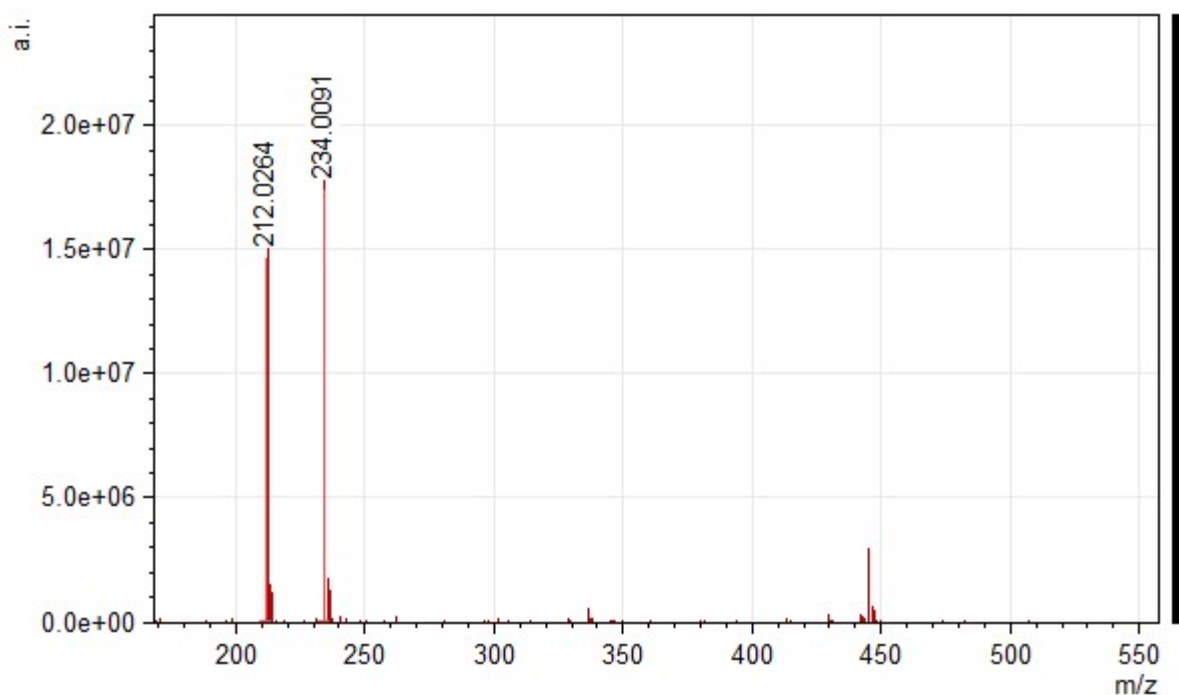


Fig. S33 ESI-MS of compound 5.

S8. References

1. Z. Lamprecht, S. G. Radhakrishnan, A. Hildebrandt, H. Lang, D. C. Liles, N. Weststrate, S. Lotz, D. I. Bezuidenhout, *Dalton Trans.* 2017, **46**, 13983.
2. N. Weststrate, Structural and electronic features of tungsten(0) and platinum(II) complexes with Fischer carbene ligands. PhD Thesis. University of Pretoria, Pretoria, 2017.
3. Y. X. Jia, X. Y. Yang, W. S. Tay, Y. Li, S. A. Pullarkat, K. Xu, H. Hirao, P. H. Leung, *Dalton Trans.* 2016, **45**, 2095.
4. A. Tyagi, S. Yadav, P. Daw, C. Ravi, J. K. Bera, *Polyhedron* 2019, **172**, 167.
5. B. G. M. Rocha, E. A. Valishina, R. S. Chay, M. F. C. Guedes Da Silva, T. M. Buslaeva, A. J. L. Pombeiro, V. Y. Kukushkin, K. V. Luzyanin, *J. Catal.* 2014, **309**, 79.
6. H. Liang, Y.-X. Ji, R.-H. Wang, Z.-H. Zhang, B. Zhang, *Org. Lett.* 2019, **21**, 2750.
7. K. H. Lee, B. Lee, K. R. Lee, M. H. Yi, N. H. Hur, *Chem. Commun.* 2012, **48**, 4414.
8. S. Schwieger, R. Herzog, C. Wagner, D. Steinborn, *J. Organomet. Chem.* 2009, **694**, 3548.
9. X. Zhao, D. Yang, Y. Zhang, B. Wang, J. Qu, *Org. Lett.* 2018, **20**, 5357.
10. S. V. Maifeld, M. N. Tran, D. Lee, *Tetrahedron Lett.* 2005, **46**, 105.
11. Z. Zhang, T. Xiao, H. Al-Megren, S. A. Aldrees, M. Al-Kinany, V. L. Kuznetsov, M. L. Kuznetsov, P. P. Edwards, *Chem. Commun.* 2017, **53**, 4026.
12. R. Cano, M. Yus, D. J. Ramón, *ACS Catal.* 2012, **2**, 1070.
13. K. Jakobsson, T. Chu, G. I. Nikonov, *ACS Catal.* 2016, **6**, 7350.
14. K. M. McWilliams, R. J. Angelici, *Organometallics* 2007, **26**, 5111.
15. R. J. Abraham, M. Canton, L. Griffiths, *Magn. Reson. Chem.* 2001, **39**, 421.
16. Z. Gan, Y. Wu, L. Gao, X. Sun, J. Lei, Z. Song, L. Li, *Tetrahedron* 2012, **68**, 6928.
17. R. Takeuchi, S. Nitta, D. Watanabe, *J. Org. Chem.* 1995, **60**, 3045.